MOLECULAR ANALYSIS OF DECAY ACCELERATING FACTOR AS A POTENTIAL SUSCEPTIBILITY FACTOR TO DEVELOPING TREATMENT RESISTANT EXTRAOCULAR MUSCLE INVOLVEMENT IN MYASTHENIA GRAVIS

HENRIETTE UWIMPUHWE BSc (Hons)

UWMHEN001

A thesis submitted to the University of Cape Town in fulfillment of the requirements for the degree of MSc (Med) in the department of Human Biology

August, 2009

I, Henriette Uwimpuhwe, hereby declare that the work on which this thesis is based is my original work (except where acknowledgements indicate otherwise) and that neither the whole work nor any part of it has been, is being, or is to be submitted for another degree in this or any other university. I empower the University to reproduce for the purpose of research either the whole or any portion of the contents in any manner whatsoever.

Signature:

Date:

Acknowledgements

I would like to express my sincere thanks to:

- My supervisor Associate Professor Jeannine Heckmann whose help, support and guidance has meant so much throughout my research.
- My co-supervisor Dr Robea Ballo for listening and teaching me so much in the laboratory. I am very grateful for her kindness, friendship and availability whenever I needed her. Thanks are also due to her for helping with the writing of this thesis.
- My co-supervisor Dr Sharon Prince for her patience, encouragement and the much appreciated help with laboratory experiments.
- The T-Box lab, especially Shaheen, Deeya, Emily, Sabina and Jade for always willing to help and enlightening up the days with laughter.
- Dr Amaal Abrahams for her invaluable advice in the writing of this thesis.
- Dr Huajian Tang for doing the site directed mutagenesis and helping me with some of the experiments.
- Ms Ingrid Baumgarten for her kindness and willingness to help in preparation of the EBV-transformed cell lines.
- Victoria van Kets for being such a friendly companion.
- My loving family whom I miss very much, my dad Jonathan, Marthe, Henri, Alida and Edmond for always encouraging me and calling every week to check on me. So much of what I have achieved I owe it to you.
- Vincent for your love, support and friendship, especially for always being there to listen and comforting me when I needed it.
- My friends outside the lab, Delphine, Josiane, Chiedza, and Lumbidzani for their friendship and moral support.
- International Brain Research Organization's Levi Montalcini Fellowship for sponsoring me. I would also like to thank Muscular Dystrophy Association of South Africa and the University of Cape Town for supporting this research.
- Last but not least, God Almighty for never leaving my side and for the good health throughout my research years.

TABLE OF CONTENTS

List of Figures

List of Tables

Abbreviations

%	percentage
ºC	degree celcius
µg	microgram
µl	microlitre
µm	micrometre
µM	micromolar
ACh	acetylcholine
AChR	acetylcholine receptor
Af-Amer	African-American
APS	ammonium persulphate
BCA	Bicichoninic acid
BLAST	basic local alignment search tool
bp	basepairs
BSA	bovine serum albumin
C	controls
$CaCl_2$	calcium chloride
cDNA	complementary DNA
cm	centimetre
cm^2	square centimetre
CO_2	carbon dioxide
CRP	complement regulatory proteins
C_T	crossing point
DAF	decay accelerating factor
DTT	dithiothreitol
dbSNP	SNP database
DLR	Dual Luciferase Reporter
DMEM	Dulbecco's modified eagle's medium
DNA	deoxyribonucleic acid
dH_2O	distilled water
dNTPs	deoxynucleotide triphosphates
E	efficiency
EAMG	experimental autoimmune myasthenia gravis
EBV	Epstein-Barr virus
EDTA	ethylenediaminetetra-acetic acid
FCS	foetal calf serum
EOM	extraocular muscle
fwd	forward
g	gram
GAPDH	glyceraldehyde-3-phosphate dehydrogenase
gDAF	GPI-anchored DAF
GPI	glycosylphosphatidylinositol
GSPEC	gDAF- specific
GUS	glucuronidase B
HCl	hydrochloric acid

HS	horse serum
kb	kilobase
KCl	potassium chloride
kDa	kilodalton
L	litre
LAR II	Luciferase assay reagent II
LB	Luria broth
LCL	lymphoblastoid cell line
LPS	lipopolysaccharide
M/A	mixed ancestry
MAC	membrane-attack complex
mg	milligram
MG	myasthenia gravis
$MgCl_2$	magnesium chloride
min	minute
ml	millilitre
mm	millimetre
mM	millimolar
mRNA	messenger RNA
Na^+	sodium ion
Mut	mutant
MW	molecular weight marker
$NaHCO_3$	Sodium hydrogen carbonate
NCBI	National Centre for Biotechnology Information
ng	nanogram
NMJ	neuromuscular junction
OD	optical density
PBS	phosphate buffered solution
PCR	Polymerase Chain reaction
PHA	phytohaemagglutinin
pmol	picamole
P/S	Penicillin- Streptomycin
qRT-PCR	quantitative real-time PCR
rev	reverse
RNA	ribonucleic acid
rpm	resolutions per minute
SA	South Africa
SANBI	South African National Bioinformatics
sDAF	soluble DAF
SDS	sodium dodecyl sulphate
SDS-PAGE	SDS- polyacrylamide gel electrophoresis
sec	second
SNP	single nucleotide polymorphism
STP	serine-threonine-proline
T_a	annealing temperature
TBE	tris borate EDTA buffer

TEMED	NNN'N'- tetramethylethylenediamine
Tm	melting temperature
Tris	tris[hydroxymethyl]aminomethane
U	unit
UCT	University of Cape Town
UK	United Kingdom
USA	United State of America
UV	ultraviolet
UWC	University of Western Cape
V	volts
WT	wild type

Abstract

Myasthenia gravis (MG) is an autoimmune disorder in which auto-antibodies directed at the acetylcholine receptors (AChR) of the neuromuscular junction (NMJ) block, alter or destroy their targets. The anti-AChR antibodies cause activation of the classical complement pathway leading to inflammatory injury at the NMJ. Decay Accelerating Factor (DAF), a member of complement regulatory proteins, prevents activation of autologous components of complement pathways. The absence of DAF, in knock-out mouse models, has been shown to significantly increase the susceptibility to experimental autoimmune MG. A previous study showed that a high proportion of South African MG patients of African genetic ancestry develop immunosuppressive therapy-resistant extraocular muscle (EOM) dysfunction. We hypothesized that these patients have deficient DAF expression in their EOMs resulting in less protection from complement injury. Sequence analysis of relevant regions of the DAF gene revealed a single nucleotide polymorphism (SNP), c.-198C>G, in the promoter region in MG patients of African genetic ancestry with severe EOM MG involvement (MG n=101; Control n= 132; Odds ratio= 6.6; p=0.009). DAF-luciferase reporter assays, using 3 different cell lines (COS-7, HT1080 and C2C12) revealed that the c.-198C>G SNP (Mut-DAF) led to an increase in DAF promoter activity (~ 2-fold) relative to that of the wild type (WT) sequence. Furthermore, quantitative real-time PCR performed on EBV transformed lymphoblastoid cell lines from four MG subjects with the c.-198C>G revealed an increase in the mRNA expression of membrane bound gDAF in the SNP cell lines compared to WT controls. Bioinformatic analyses revealed that the SNP led to the loss of a putative Sp1 transcription factor binding element within the promoter region of DAF. Co-transfections of either the WT- or Mut-DAF with pCMV-Sp1 and/or empty vector showed similar results suggesting that the putative Sp1 site lost by the SNP was not crucial for basal DAF regulation. However, the c.-198C>G SNP did not show the expected lipopolysaccharide (LPS)-induced DAF mRNA up-regulation in cell lines from four patients carrying this SNP. Results from this study therefore suggest that the c.-198C>G associated with a severe EOM outcome in MG impairs normal transcriptional regulation of the DAF gene in response to an immune stress stimulus such as LPS. The loss of the Sp1 binding site may result in inadequate upregulation of DAF expression at critical periods during the autoimmune response in MG with less protection of the EOM against complement-mediated damage.

CHAPTER 1: LITERATURE REVIEW

1.1 Myasthenia gravis

Myasthenia gravis (MG) is an autoimmune disorder in which auto-antibodies are directed at the acetylcholine receptors (AChRs) at the neuromuscular junction (NMJ). This leads to neuromuscular transmission failure and weakness (Kaminski, 2003). MG was initially recognised in the 1600s when it was known as fatiguable weakness disorder (reviewed in Conti-Fine et al., 2006). The term myasthenia gravis was introduced in the late 1800s by combining the two Greek words of muscle and weakness, that is myasthenia, and adding the Latin word, gravis, which means severe (Keesey, 2002).

MG is characterised by varying degrees of skeletal muscle weakness that increases during periods of activity and improves after periods of rest. The muscles that are usually affected include those controlling eye and eyelid movement, and limb movements. In addition, muscles that control breathing, chewing, swallowing, talking and facial expression may also be affected (reviewed in Conti-Fine et al., 2006). The extraocular muscles (EOMs) usually present as the initial symptom and in 90% of the patients the symptoms progress to other skeletal muscles mentioned. Therefore, MG is classified as ocular MG (when symptoms are limited to the EOMs) and generalized MG (symptoms are present in EOMs and other voluntary muscles) (reviewed in Conti-Fine et al., 2006).

Two types of MG exist, namely seropositive and seronegative. The majority of MG patients (85-90%) are seropositive as they possess antibodies against the AChRs at the NMJs (Bateman et al., 2005). Patients without detectable anti-AChR antibodies, however, are said to have seronegative MG and may have antibodies directed against other proteins found at the NMJ. The incidence rate of seropositive MG in South Africa is similar to that of other developing countries but is lower than that of developed countries. However, the incidence of seropositive MG in Cape Town, South Africa, was found to be 11.2 per million per year, comparable to that of developed countries (Bateman et al.,

2005). These results suggested underreporting in areas of South Africa where access to health care may be suboptimal (Bateman et al., 2005).

Studies from both MG patients and experimental autoimmune MG (EAMG) in animals, showed that the AChR antibodies act by directly blocking the AChR function, accelerating AChR degradation, or initiating complement-mediated damage at the NMJ (Zhou et al., 2007). The EAMG model was established in animals through immunization with purified solubilised AChR (Lennon et al., 1978) or by passive transfer of anti-AChR antibodies (Piddlesden et al., 1996).

1.2 The neuromuscular junction and MG susceptibility of extraocular muscles

The NMJ is the contact between the terminal nerve endings and the muscle fibres and lacks the protection that the blood-brain barrier provides for synapses in the central nervous system (Walton et al., 1994). The axon of each motor neuron divides into many branches as it approaches the synaptic bouton and each of these endings forms a NMJ with a single muscle fiber (**Figure1.1**). The terminal end of the axon contains synaptic vesicles that are filled with the neurotransmitter, acetylcholine (ACh), which is released when the action potential arrives at the axonal terminal. The postsynaptic membrane of the NMJ is highly folded and the AChRs are present on the crests of these folds. ACh diffuses across the synaptic cleft and attaches to the AChRs on the postsynaptic membrane causing the opening of the Na+ channels resulting in the initiation of depolarization along the muscle fibre.

The NMJs of different muscles have varying properties and this may influence its susceptibility to MG (Hughes et al., 2006). For example, the NMJs of the EOMs, which control the movement of the eye, are more susceptible to MG than other muscles but the exact reason for this is still not clear. The EOMs constitute a unique group of six small skeletal muscles with a distinctive fiber type composition (Khanna et al., 2003). The NMJs of the EOMs are easily fatigued because of their very high neuronal firing frequency (Kaminski et al.,

2004). These NMJs also have less prominent synaptic folds and fewer postsynaptic AChRs and Na+ channels (Khanna and Porter, 2002). It is also speculated that the NMJs of the EOM may be more susceptible to MG because they express less membrane-bound complement regulatory proteins compared to limb muscles hence less protection from complement-mediated damage (Kaminski et al., 2004; Conti-Fine et al., 2006).

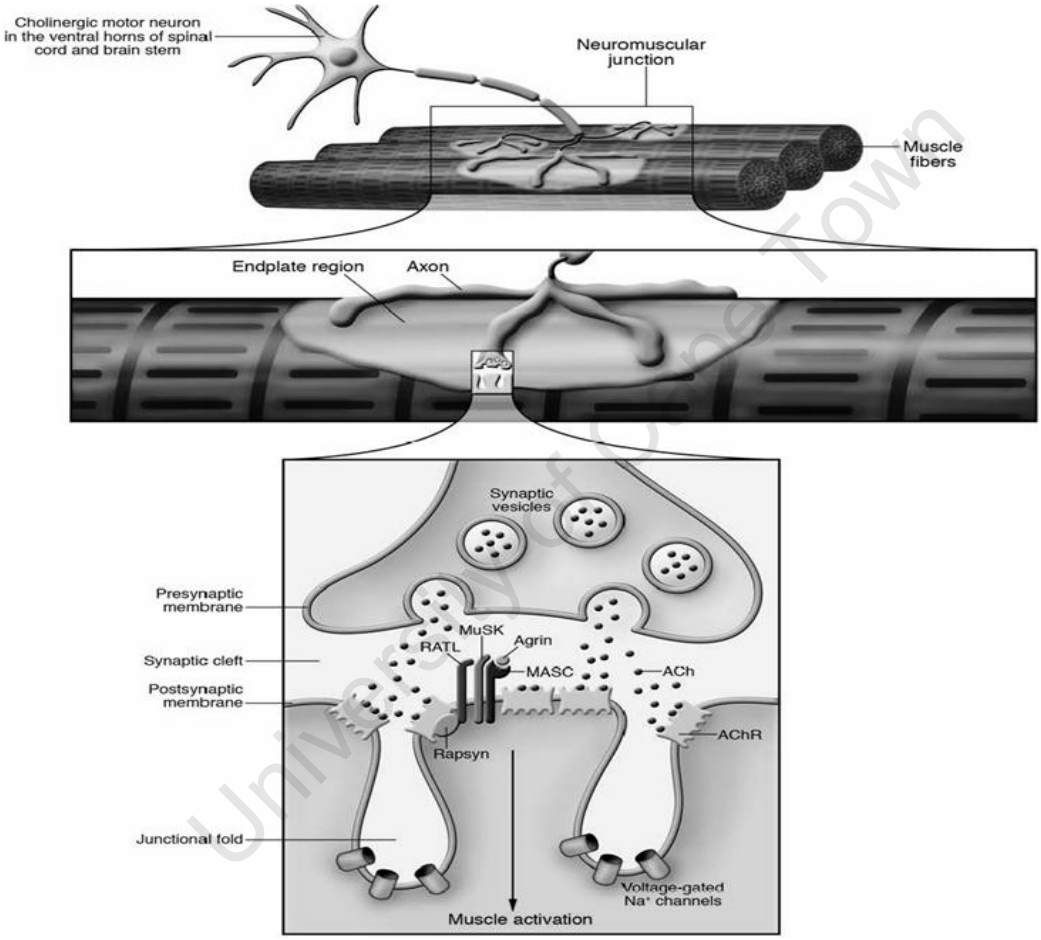

Figure1.1: Structure of the neuromuscular junction (NMJ). The axon of each motor neuron divides into many branches forming synaptic boutons and each of these endings forms a NMJ with a single muscle fiber. ACh diffuses across the synaptic cleft and attaches to the AChRs on the postsynaptic membrane causing the opening of the Na+ channels and initiates the depolarization along the muscle fiber. (Adapted from Conti-Fine et al., 2006).

1.3 The complement system and relevance to MG

The complement system is a cascade of biochemical reactions composed of over 30 different serum and membrane proteins, which help to clear pathogens from the body and help the immune cells in fighting cancers and infections. This is done through cell lysis of pathogens, enhancement of phagocytosis and the attraction of inflammatory cells (Kohl, 2006; Walport, 2001). Complement can be activated by three different pathways, namely, the classical, alternative and lectin pathways (**Figure 1.2**). All three pathways lead to the formation of proteolytic enzymes known as C3 convertases, which mediate the cleavage of the C3 protein into C3a and C3b (Kim and Song, 2006; Walport, 2001). This is followed by a series of activation steps and the generation of a number of proteins which lead to the formation of the membrane-attack complex (MAC) that causes cell destruction.

In MG, the classical complement pathway is most relevant as it is activated by the pathogenic auto-antibodies attacking the AChRs on the postsynaptic membrane. Ultimately, this results in the formation of the MAC which leads to the damage of the postsynaptic surface of the muscle and contributes to failure of neuromuscular transmission (Soltys et al., 2008).

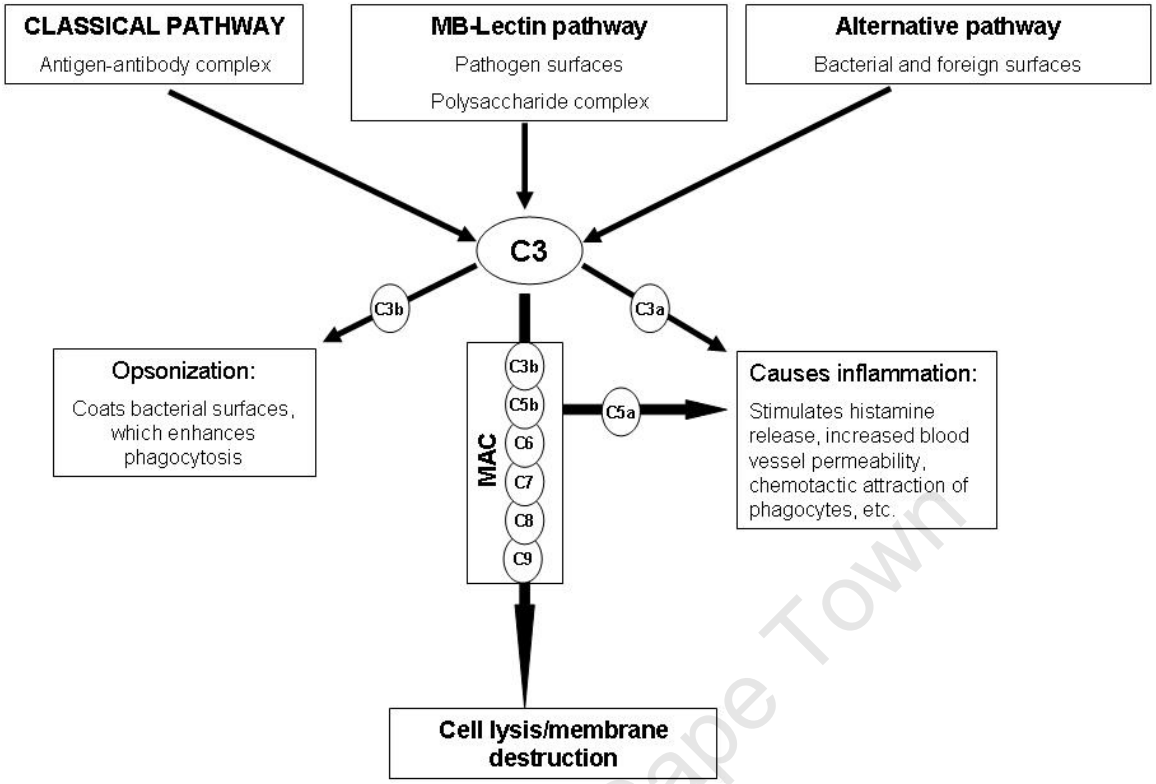

Figure 1.2: Complement pathways, events and results of an activated complement system. There are three pathways involved in the complement system: classical, mannose-binding (MB)-lectin and alternative. The classical pathway is activated by antigen-antibody complex. For MG, the classical pathway is most relevant because of its activation by the antibodies that attack the acetylcholine receptors (AChRs). All three pathways converge on C3 resulting in its cleavage into C3a and C3b fragments. These proteins go through a series of events which leads to the formation of the membrane-attack complex (MAC) which is a common terminal pathway that causes cell lysis.

There is ample evidence indicating that complement is the primary cause of damage at the NMJ in MG. Complement activation fragments C3, C9 and the MAC have been found at the NMJs in MG patients (Engel et al., 1979, Nakano and Engel, 1993; Sahashi et al., 1980, Fazekas et al., 1986). Furthermore, the C3 component was shown to be localised at the motor end-plate in animals with experimental autoimmune MG (EAMG), (Sahashi et al., 1978). In another study, cobra venom factor, known to prevent or reduce complement, was used to treat rats with EAMG (Lennon et al., 1978). Piddlesden et al. (1996) also showed that the potent complement regulatory molecule, soluble complement receptor 1, protects against the induction of EAMG.

The complement system has to be tightly regulated to avoid damage of the body's own cells. To prevent injury caused by activated complement a group of proteins known as complement regulatory proteins (CRPs), are ubiquitously expressed on the surfaces of almost all cell types (Miwa and Song, 2001; Kim and Song, 2006).

1.4 Complement regulatory proteins (CRPs)

Several CRPs have been characterized in humans including; decay accelerating factor (DAF) or CD55, a 70 kDa glycolipid-anchored membrane-bound protein which regulates complement activity by preventing the formation of C3 and C5 convertases and accelerating their decay (Lublin and Atkinson, 1989); membrane cofactor protein (MCP) or CD46, which is a 60 kDa protein that mediates cleavage of C3b and C4b (Liszewski et al., 1991; Barilla-LaBarea et al., 2002); complement receptor 1 (CR1) or CD35, is a transmembrane receptor (190-280 kDa) that binds and processes C3b and C4b convertases (Ahern and Fearon, 1989; Murray et al., 2000); CD59, also known as protectin, is a 18 to 20 kDa membrane-anchored protein that inhibits the formation of the terminal MAC on complement by binding to C8 and C9 and disrupting the C8:C9 ratio in the MAC (Okada et al., 1989; Rollins and Sims, 1990). Mice have also been shown to express a rare transmembrane protein complement-receptor 1-related gene/protein y (Crry) (Miwa and Song, 2001) (**Figure 1.3**) that has similar activity to that of MCP (Kim and Song, 2006).

1.4.1 Structure and function of CRPs

DAF and CD59 are attached to the cell membrane by a glycosylphopshatidylinositol (GPI)-anchor, whereas MCP, CR1 and Crry are inserted in the membrane via transmembrane domains (Miwa and Song, 2001; Kim and Song, 2006) (**Figure 1.3**).

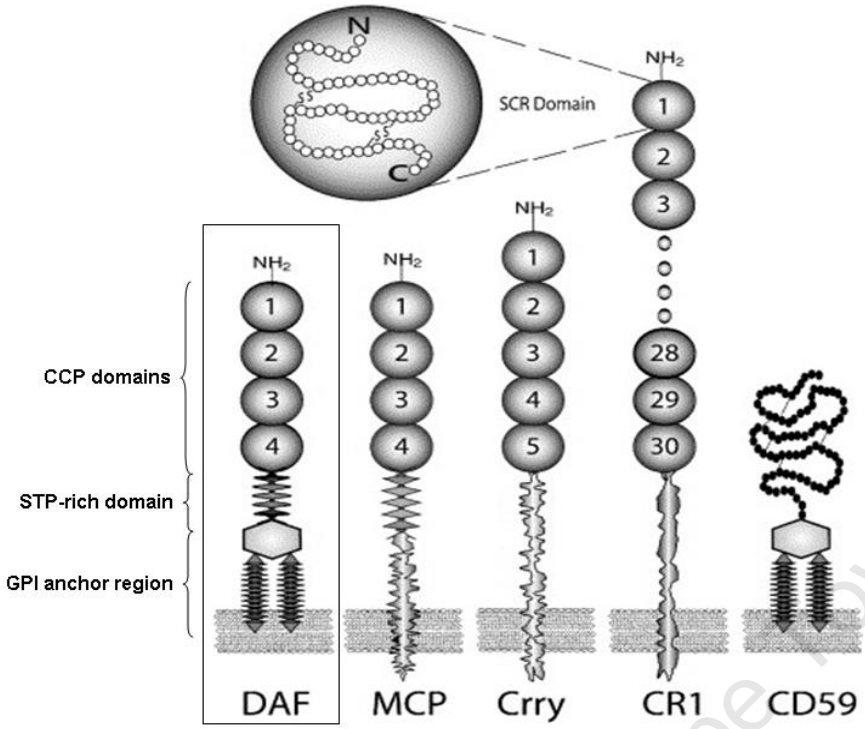

Figure 1.3: Structures of complement regulatory proteins, human DAF, MCP, CR1, CD59 and mouse Crry. DAF and CD59 are attached to the cell membrane by a glycosylphosphatidylinositol (GPI)-anchor, whereas MCP, CR1 and mouse Crry are attached via transmembrane domains. DAF and MCP have four complement control protein (CCP) domains and contain a STP-rich region between the CCP domains and the GPI-anchor or transmembrane domain (Kim and Song, 2006).

Structurally, DAF, MCP, Crry and CR1 belong to a family of genes that regulates complement activation. They contain variable numbers of complement control protein (CCP) domains, also known as short consensus repeat domains. These CCP domains consist of approximately 70 amino acids with 4 conserved cysteine residues that form disulphide bonds (Kim and Song, 2006). DAF and MCP contain four CCP domains, human CR1 has 30 CCP domains and mouse Crry has five CCP domains (Miwa and Song, 2001) (**Figure 1.3**). CD59, the smallest protein of CRPs, does not contain any CCP domains, but its extracellular domain consists of approximately 70 amino acids with five disulphide bonds between the cysteine residues (Kim and Song, 2006) (**Figure 1.3**). A serine-threonine-proline (STP)-rich region between the CCP domains and

the GPI-anchor or transmembrane protein is present in DAF and MCP, respectively (Kim and Song, 2006) (**Figure 1.3**).

1.4.2 Comparison between human and mouse CRPs

A number of CRPs in humans correspond to those characterised in mice although several differences have been identified in the composition and expression patterns of their membrane CRPs (Miwa and Song, 2001). Crry is widely expressed in mice whereas MCP is restricted to the testis. Mice also differ from human in that their DAF and CD59 genes are duplicated into daf-1 and daf-2, cd59a and cd59b genes, respectively (Spicer et al., 1995; Qian et al., 2000; Qin et al., 2001). Mouse daf-1 and cd59a, the human DAF and CD59 homologues, are ubiquitously expressed and membrane-bound through their GPI-anchors (**Figure 1.3**), whereas daf-2 and cd59b are transmembrane proteins which are only expressed in the testis and splenic dendritic cells (Kaminski et al., 2004; Harris et al., 2003).

DAF is one of the CRPs that has been implicated in MG. Experiments done in mice showed that the Daf1 knockout mice with deficient neuromuscular Daf1 protein showed enhanced susceptibility to passively induced MG compared to control mice (Lin et al., 2002). CD59 has also been implicated in MG, however, mouse experiments have shown that DAF was more crucial in muscle protection against EAMG-associated complement injury (Kaminski et al., 2006). Daf1 knock out mice compared to their wild type littermates showed more susceptibility to EAMG induction and suffered more severe complement injury than the CD59 knockout mice which showed minimal weakness compared to wild type (Kaminski et al., 2006; Lin et al., 2002).

1.5 Decay accelerating factor (DAF)

DAF or CD55 was first described in human erythrocytes by Hoffmann (1969) and was later isolated and characterised by Nicholson-Weller et al. (1982). The gene encoding DAF is located on chromosome 1, band q32 in the complement-

regulatory locus together with other complement regulating proteins (Lublin et al., 1987).

There are two major isoforms of DAF in humans, a glycosylphosphatidylinositol (GPI)-anchored form (gDAF), and a soluble form, sDAF (Medof et al., 1987), with five minor variants (Osuka et al., 2006). All these isoforms are generated from the same gene by alternative splicing (Caras et al., 1989). The gDAF isoform is ubiquitously expressed on almost all peripheral blood cells (Kinoshita et al., 1985; Nicholson-Weller et al., 1985), epithelial and endothelial cells (Asch et al., 1986; Medof et al., 1987), unlike the sDAF which is expressed in the body fluids and extracellular matrix at much lower levels (Medof et al., 1987).

The function of DAF is to protect host cells from activation of autologous complement on their surface. This is achieved by preventing the formation of new, and accelerating the decay of the classical and alternative C3 and C5 convertases (Lublin and Atkinson, 1989; Nussewzweig, 1984). Previous studies have also identified DAF as a negative modulator of T cell immunity (Liu et al., 2005; Heeger et al., 2005). DAF was also shown to have other noncomplement-related functions, such as acting as a cellular ligand of CD97 (CD97-CD55) which is a member of the epidermal growth factor family (Hamann et al., 1996). The CD97-CD55 complex also appears to regulate T-cell effector function (Abbott et al., 2007).

1.5.1 Structure and function of DAF

The functional sites of DAF are contained within four N-terminal CCP domains encoded by exons 2 to 6 (Post et al., 1989) (**Figure 1.4**). The four CCPs are held above the surface of the membrane by the heavily glycosylated STP-rich stalk, encoded by exons 7, 8 and 9. The length of exons 7, 8 and 9 vary greatly, encoding 42, 27 and 7 amino acids, respectively, but approximately equal amounts of serine and threonine residues (40 to 44%) (Post et al., 1989). The soluble isoform, sDAF, differs from the GPI-anchored gDAF in that it includes encoding from exon 10 and excludes exon 14 that encodes for the GPI-anchor,

and is found in bodily fluids and extracellular matrix (Medof et al., 1987). Three of the minor variants vDAF1, vDAF2 and vDAF3 include exons 11, 12 and 13 respectively, and they lack the GPI-anchor just like the sDAF (Osuka et al., 2006).

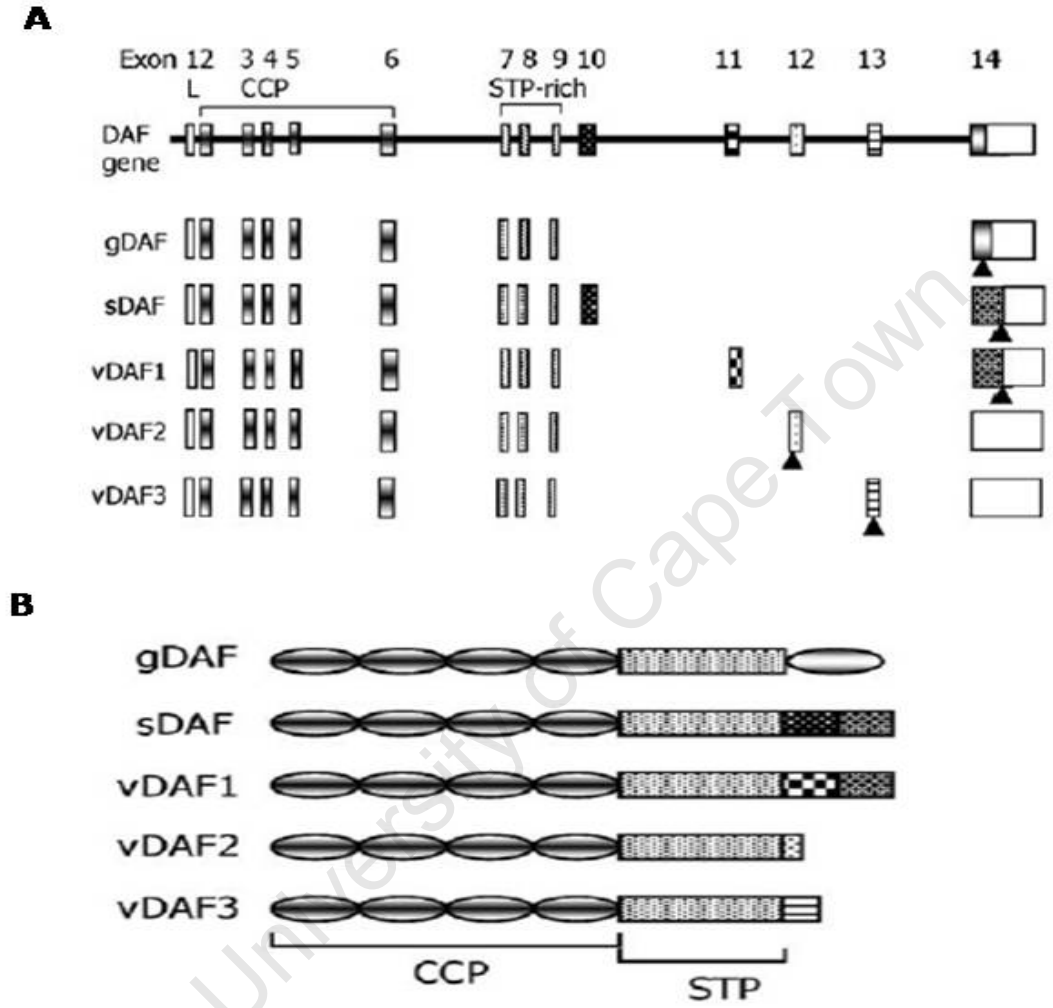

Figure 1.4: **A)** Schematic diagram showing isoforms of the human DAF gene, namely gDAF, sDAF, vDAF1, vDAF2 and vDAF3. The boxes represent the exons of the DAF gene, showing that exons 2 to 6 encode for the CCP domains, exons 7 to 9 encode for the STP rich domain and exons 10 to 14 encode the C-terminal region. The arrowheads below the boxes show the position of the stop codons in the cDNAs. **B)** Schematic diagram of the domain structures. Each domain is shown by a different pattern, which in turn corresponds to the exon with the same pattern. Adapted from Osuka et al., 2006.

The anchorage of gDAF on the membrane is facilitated by the GPI anchor attachment site encoded by the last exon 14 (Osuka et al., 2006) which also

encodes the 3` untranslated region (Post et al., 1989). The GPI membrane attachment is directed by the carboxyl (COOH)-terminal signal, Serine-319, which is the cleavage site at the COOH-terminus (Caras, 1991).

The remaining 2 minor variants, vDAF4 and vDAF5 contain either part of or the full intron 7 in their mRNA, and possess the GPI-anchor as the gDAF isoform (Osuka et al., 2006). The active sites of DAF for the classical and the alternative complement pathways are different (Coyne et al., 1992). It was shown by Coyne et al. (1992) using deletion constructs that the CCP1 did not affect the function of DAF on complement whereas the deletion of the CCP2, 3 and 4 individually, completely abolished the function of DAF. In addition, it was shown that whereas inhibition of both the classical and the alternative pathways require the regulatory function of the CCP2 and 3 (Coyne et al., 1992; Brodbeck et al., 1996; Brodbeck et al., 2000; Kuttner-Kondo et al., 2001), the CCP4 is necessary for the regulation of the alternative complement pathway function only. The STP-rich region has been shown to prevent rapid proteolysis of the DAF molecule as it is heavily glycosylated and has a critical spacer function that holds DAF further away from the plasma membrane (Coyne et al., 1992).

1.5.2 Regulation of *DAF* gene expression

DAF expression has been shown to be modulated by cytokines, for example IL-1, IL-6, TNF-alpha, TGF-beta 1, IFN-gamma, prostaglandins and tissue-specific factors suggesting that regulation of DAF expression is tissue- and cell-type specific and affected by inflammation (reviewed in Cauvi et al., 2006). The primary regulation of DAF has been demonstrated to be at a transcriptional level (Thomas and Lublin, 1993; Kendall et al., 1996).

The *DAF* promoter has been shown, in both human and mouse, to lack the TATA and CCAAT boxes (Thomas and Lublin, 1993; Cauvi et al., 2006) and to contain a GC-rich domain, which is a common feature of TATA-less promoters (reviewed in Cauvi et al., 2006). Furthermore, TATA-less promoters frequently contain several transcriptional start sites, as is the case for house-keeping genes which are also TATA-less and GC-rich (reviewed in Thomas and Lublin, 1993).

Ewulonu et al. (1991) identified the main transcriptional start site of *DAF* to be located 82 bp upstream of the ATG codon, whereas Thomas and Lublin (1993) found several transcription start sites in a 10 bp region located 87 bp upstream of the ATG codon. Deletion analyses of the *DAF* promoter have shown that the promoter region contains both enhancer and repressor elements that influence the regulation of the *DAF* gene (Cauvi et al., 2006; Thomas and Lublin, 1993).

1.5.3 Relevance of DAF in other disorders

Several studies have implicated DAF in a number of inflammatory disorders although its exact role is not fully understood. Complement fragments, C3b, were detected at the site of injury in chronic inflammatory bowel diseases in humans (Halstensen et al., 1992; Ueki et al., 1996) possibly implicating reduced DAF expression. Individuals with the Cromer Inab phenotype of blood group antigens have been found to develop inflammatory bowel diseases due to polymorphisms within the DAF gene resulting in low or no DAF expression (Daniels et al., 1998; Tate et al., 1989; Lublin et al., 1994; Lin et al., 2004). This disorder results from complement injury to the gastrointestinal tract tissue cells (Lin et al., 2004).

Experiments performed in an experimental model of inflammatory bowel disease also showed that DAF-deficient mice were more susceptible to epithelial injury in their distal colon induced by dextran sulfate sodium and had delayed tissue healing (Lin et al., 2004). Moreover, Miwa et al. (2007) also showed that DAF expression was particularly important in reducing local skin inflammation in the murine model of human systemic lupus erythematosus.

In paroxysmal nocturnal hemoglobinuria, patients have little or no membrane bound DAF or CD59 on their erythrocytes. In this acquired condition complement leads to the destruction of red blood cells in the blood stream due to a defect in the GPI anchor (Rosse and Nishimura, 2003; Yazer et al., 2006). Finally, DAF was also found to be down-regulated in individuals and mouse models with dysferlin-deficient muscular dystrophy (Wenzel et al., 2005). In this study it was shown that the reduced DAF expression led to increased susceptibility of myotubes to complement attack.

1.6 Background relevant to this study

The University of Cape Town-MG clinic has reported racial differences in the phenotype of MG and the response of these MG patients to standard immunosuppressive treatment (Heckmann et al., 2007). Proportionately more individuals of African ancestry developed a severe ocular phenotype characterised by treatment-resistant complete ophthalmoplegia and ptosis, in which all the EOMs and eyelids are paresed (Heckmann et al., 2007). **Figure 1.5** is a photograph of one of the patients with complete ophthalmoplegia and ptosis. In the present study we investigated whether these phenotypic differences were related to a reduction of DAF expression associated with genetic polymorphisms or mutations in the DAF molecule. It was hypothesised that DAF expression may be lower than normal or not properly upregulated during "inflammatory stress" resulting in inadequate complement protection in the EOM's of the subgroup of MG patients tested.

Figure 1.5: Photograph of MG patient with severe eye involvement (with permission from the patient) (Heckmann et al., 2007).

1.7 Association studies

Genetic association studies have been widely used to study whether genetic variants in populations contribute to the susceptibility of complex disorders (Campbell and Rudan, 2002). The rationale for genetic association studies is to determine whether a genetic variant, such as a single nucleotide polymorphism (SNP), is associated with a disease or trait statistically, and to identify if the allele

frequencies are different between case studies (diseased individuals) and healthy controls from the same population group (Rodriguez-Murillo and Greenberg, 2008). An association can be expected between a disease trait and a genetic variant if the variant either has a direct functional effect on the phenotype or if it is in linkage disequilibrium (LD) with a pathogenic mutation or functional polymorphism. LD is when two or more loci on a chromosome are more likely to segregate together in meiosis due to physical proximity to each other on a chromosome (Cardon and Bell, 2001; Rodriguez-Murillo and Greenberg, 2008). Once association of a genetic polymorphism has been established in one population it should be repeated in another (Campbell and Rudan, 2002) Experiments are then carried out to investigate the functional importance of the variants and how it relates to the phenotype (Luretta, 2008). A number of SNPs has been shown to play essential roles in susceptibility to several complex multifactorial disease traits, including type I diabetes and Graves' autoimmune disease (Knight, 2004).

The estimation of SNP allele frequencies is a simple and cost-effective approach in genetic association studies (Rodriguez-Murillo and Greenberg, 2008). A difference in the allele frequencies of the SNP between the patients and the controls from the same population would indicate that the genetic marker may increase the likelihood of the disease trait, or be in LD with a disease causing SNP (Rodriguez-Murillo and Greenberg, 2008; Cardon and Bell, 2001).

1.8 Study objectives

The main objective of this study was to investigate the involvement of DAF in the increased susceptibility of African (or recent admixture) MG patients in the development of treatment resistant extra ocular muscle (EOM) paralysis.

This was achieved by:

I. Examining critical areas of the DAF gene for mutations in exons as well as the promoter region.

II. Determining the functional importance of genetic change(s) by using site-directed mutagenesis to mimic these changes.

III. Investigating whether the membrane-bound gDAF expression is altered in the peripheral blood lymphocytes and the lymphoblastoid cell lines from the MG patients using real-time Polymerase Chain Reaction and western analyses.

CHAPTER 2: MATERIALS AND METHODS

2.1 Decay-accelerating factor (DAF) genotyping

2.1.1 Subpopulations of patients and controls

This study was undertaken on 136 patients and 167 controls **(Table 2.1)**. Unselected patients attending the UCT-MG clinic were invited to participate and after obtaining informed consent, EDTA blood for DNA extraction was collected. The severity of extra-ocular muscle (EOM) dysfunction (at rest) of the patients was assessed and quantified according to the scoring method described by Heckmann et al. (2007). Patients belonged to the White, Mixed-Ancestry (M/A) or Black subpopulations of South Africa. Whites are mostly of European origin, the Black subpopulation is composed of indigenous Black Africans while the M/A (also known as Coloured) subpopulation is composed of an admixture of European, African, Indian, Malay and Khoi San. Racially matched control DNA was taken from DNA samples collected during a previous study (Heckmann et al., 2001) with permission to use the samples for subsequent unrelated genetic studies, as approved by the UCT Research Ethics Committee permission.

Table 2.1: The total number of patients and controls screened in the three racial groups of patients and controls

	MG patients	Controls
White	34	35
Mixed ancestry	72	84
Black	30	48
Total	136	167

2.1.2 Primer designing

For mutation screening in genomic DNA using conventional PCR, oligonucleotide primers were designed to be intronic, flanking the exons and the intron/exon junctions to be sequenced. The oligonucleotides were derived from the DAF

sequence, Genebank RefSeq-file NM_000574, in the human genome database (www.ncbi.nlm.nih.gov/entrez) and are listed in **Table 2.2**. Generally, the primers used were 18 to 26 nucleotides long, had 45 to 55% GC contents and the differences between melting temperatures of the sense and the antisense primers were less than 5ºC. Primers capable of being self-complementary or complementary to each other in the reaction mixture were avoided.

For RNA expression analysis using quantitative real time PCR, primers were designed to specifically amplify the membrane-bound gDAF and exclude the other major isoform, sDAF, and the minor isoforms, vDAF 1 to 5. This was achieved by designing the primers so that the reverse primer spanned the exon 9/ exon 14 junction as shown in the sequence below (**Figure 2.1**). This primer pair is referred to as Gspec (for gDAF-specific) and is shown in boxes in **Figure 2.1** which shows the Gspec forward primer (5'- GGATTCACCATGATTGGAGAGC- 3') in exon 6 and the Gspec reverse primer (5'- TGTGCCCAGATAGAAGAC- 3') spanning the exon 9 / exon 14 junction. The oligonucleotide primers for the house-keeping genes, glucuronidase B (GUS) and glyceraldehyde-3-phosphate dehydrogenase (GAPDH) were obtained from Quantitect (QIAGEN, USA).

GTAACGTATGCATGTAATAAAGGATTCACCATGATTGGAGAGCACTCTATTT
ATTGTACTGTGAATAATGATGAAGGAGAGTGGAGTGGCCCACCACCTGAAT
GCAGAGGAAAATCTCTAACTTCCAAGGTCCCACCAACAGTTCAGAAACCTAC
CACAGTAAATGTTCCAACTACAGAAGTCTCACCAACTTCTCAGAAAACCACC
ACAAAAACCACCACACCAAATGCTCAAGCAACACGGAGTACACCTGTTTCCA
GGACAACCAAGCATTTTCATGAAACAACCCCAAATAAAGGAAGTGGAACCAC
TTCAGGTACTACCCGTCTTCTATCTGGGCACACGTGTTTCACGTTGACAGGT
TTGCTTGGGACGCTAGTAACCATGGGCTTGCTGACTTAG

Figure 2.1: CCDS 31006.1 sequence obtained from CCDS Database, NCBI. The blue and the black colours show the alternating exons. The forward (sense) primer is in exon 6 and the reverse (antisense) primer is at the exon 9/ exon 14 junction. Primer sequences are shown in boxes.

Table 2.2: Primer sequences (sense and antisense) used to amplify the different regions of the *DAF* gene.

Oligonucleotides	Sequence	Annealing temperature	Number of bases
Promoter sense	5`-ACACCCCGTTTGTTTTACG-3`	60°C	20
Promoter antisense	5`-GCACAACAGCACCAGCAG-3`	60°C	18
Exon 3 sense	5`-TTGCTGCTTTTGTTAATACTTTTAGG-3`	56°C- 60°C	26
Exon 3 antisense	5`-TATTTCCCCCAAACACCAGA-3`	56°C- 60°C	20
Exon 4 sense	5`-CATAGTTACCTTCTTTGTGTGTATGC-3`	63°C	26
Exon 4 antisense	5`-GTCCTAATTTGTTTTCTCATTTCC-3`	63°C	24
Exon 5 sense	5`-CCTGGAGAATTTGAGGAAAGT-3`	63°C	21
Exon 5 antisense	5`-GCCTCACAATCTGAGTGCTT-3`	63°C	20
Gspec sense	5`-GGATTCACCATGATTGGAGAGC-3`	50°C- 53°C	22
Gspec antisense	5`-TGTGCCCAGATAGAAGAC-3`	50°C- 53°C	19

2.1.3 Measuring DNA concentration

The concentration of extracted DNA was measured using a NanoDrop ND-1000 UV-visible spectrophotometer (NanoDrop Technologies, USA). The NanoDrop software displays the concentration in ng/µl and an estimation of the purity of DNA is assessed by 260/280 ratio. A ratio of 1.8 - 2.0 is accepted as pure for DNA.

2.1.4 Conventional polymerase chain reaction (PCR)

Genomic DNA was extracted from whole blood from patients and controls using the Genomic DNA purification kit (PUREGENE® DNA Purification System, Gentra Systems, USA) according to the manufacturer's protocol. Generally, PCR was performed in a volume of 25 µl using 100 ng of template DNA and a final concentration of 10 pmol sense and antisense oligonucleotides, 200 µM dNTPs, 1x Taq polymerase buffer, 1.5 mM $MgCl_2$ and 0.1 – 1 U Taq DNA polymerase **(Table 2.3)**.

PCR was performed under the following conditions: initial denaturation at 94°C (5 minutes) followed by 25 amplification cycles comprising denaturation at 94°C (30 seconds), annealing at 60°C (30 seconds) temperature which varied from 50°C to 63°C according to oligonucleotides corresponding to individual

regions of the DAF gene **(Table 2.2)**, extension of 72°C (30 seconds), followed by a final extension at 72°C (7 minutes) in a 2720 Thermal Cycler (Applied Biosystems, USA).

Some parameters were altered slightly in several PCR attempts, to optimize the PCR reactions. These included the initial amount of DNA template (50 ng – 200 ng), $MgCl_2$ concentration (1.5 mM – 3 mM), the annealing temperature (50°C – 63°C), the type of commercial *Taq Polymerase* enzymes, *GoTaq* (Promega, USA) and *BioTaq* (Bioline Ltd, UK), and buffers (GoTaq, BioTaq and Failsafe (Epicentre Biotechnologies, USA)).

Table 2.3: Summary of the optimized PCR reaction mixture set up for *DAF* gene amplification

Reagent	BioTaq	GoTaq	Failsafe
Template DNA (100 ng/µl)	100 ng	100 ng	50 ng
Forward primer (20 µM)	10 pmols	10 pmols	10 pmols
Reverse primer (20 µM)	10 pmols	10 pmols	10 pmols
dNTPs	200 µM	200 µM	200 µM
5 x GoTaq Buffer	-	1 x	-
GoTaq DNA polymerase	-	1 unit	1 unit
2 x Failsafe Buffer	-	-	1 x
10 x BioTaq Buffer	1 x	-	-
BioTaq DNA polymerase	1 unit	-	1 unit
$MgCl_2$ (50 mM)	1.5 mM	-	-

2.1.5 Agarose gel electrophoresis

The size of the amplified PCR product was checked by electrophoresis on a 2% agarose gel. A total volume of 8 µl of sample was loaded per well containing 5 µl of PCR product mixed with 3 µl of agarose loading dye. In this study, the loading dye was spiked with the fluorescent stain, SYBR gold (Invitrogen, USA) in the

ratio 1:2000 (appendix A), for visualization on a UV transluminator. A 100 bp molecular weight marker (appendix B) was loaded on each gel together with the PCR products.

2.1.6 Sequencing

PCR products were sequenced either in one or both forward and reverse directions, using the same oligonucleotides used for PCR amplification. The sequencing reactions were performed using the BigDye® terminator cycle version 3.1 sequencing kit (Applied Biosystems, USA). Briefly, the reaction was composed of 10 µM of oligonucleotide, 1x reaction buffer, 2 µl of termination mix and 2 µl of PCR product in a total volume of 20 µl. The cycling conditions used were 96°C for 5 minutes followed by 25 cycles of 95°C for 30 seconds, 50°C for 15 seconds and 60°C for 4 minutes.

After the cycle sequencing reaction the products were cleaned by ethanol precipitation (Appendix A), air-dried then mixed with Hi-Di™ formamide (Applied Biosystems, USA) and heat denatured prior to electrophoresis on an acrylamide gel. The DNA sequences were read on the ABI Prism™ 3100 automated sequencer (Applied Biosystems, USA). Analysis was performed using ABI™ DNA Sequencing Analysis Software version 3.7. The sequences obtained were also confirmed manually and analyzed for any changes by aligning them with the known reference sequence using the Clustal Alignment facility in BioEdit version 7.0.0.

2.1.7 Statistical analysis

Allele and genotype frequencies were compared between groups using 2 x 2 tables to obtain a Yates corrected Chi-square 2-tailed p-value; if a cell value was <5 the Fisher-exact test was used (http://www.openepi.com). Odds ratios were determined relative to control populations. $P<0.05$ was considered statistically significant.

2.2 Amplification of DNA constructs

2.2.1 Plasmid constructs

The decay accelerating factor (DAF) promoter region (-724 to +80) cloned as a Bgl II and Hind III fragment in the pGL3-basic firefly luciferase reporter vector was kindly donated by Ray DuBois (Holla et al., 2004) and will be referred to as WT-DAF throughout this thesis. Site directed mutagenesis was performed, using the WT-DAF reporter construct as a template, to mutate the C at position -198 to G (performed by Dr Huajiang Teng, UCT) and this construct will be called Mut-DAF throughout this thesis.

2.2.2 Making competent cells

DH5α*E. coli* cells were inoculated into 5 ml of Luria Broth (LB) (appendix A) and incubated overnight at 37°C with shaking. One ml of this culture was then used to inoculate 100 ml of LB and cells grown for 2 to 3 hours until cell growth reached the log phase (OD_{595} = 0.6). Cells were centrifuged at 1800 x g for 10 minutes at room temperature (Centrifuge 5810R, Eppendorf, Germany); the bacterial pellet re-suspended in 100 mM Calcium chloride ($CaCl_2$) solution and incubated on ice for 1 hour. Following centrifugation, the supernatant was discarded and 1 ml of $CaCl_2$ was used to re-suspend the pellet. $CaCl_2$ creates small holes in the cell wall of the bacteria that allow for the entry of foreign DNA but causes the cells to be very fragile and care was taken in successive processes so as not to permanently damage the cells. A 100 µl of competent cells were either used immediately for DNA transformation or they were frozen in autoclaved glycerol at -70°C for long term storage.

2.2.3 Ampicillin agar plates

All plasmids used in this study carried the ampicillin resistance gene. Ampicillin (50 µg/ml) was added to 1.5% bacterial agar (prepared in LB) which was poured into 10 cm dishes to a volume of 20 ml per dish. The agar was allowed to set at room temperature and then dried overnight at 37°C.

2.2.4 Transformation

To a 100 µl of competent cells, 5 µl of DNA plasmid solution was added and then incubated on ice for 10 minutes. Cells were heat-shocked at 42°C for 1 minute, to allow the bacteria to take up the DNA constructs. Cells were then incubated on ice for 2 minutes, after which 300 µl of antibiotic-free LB was added and the cells incubated at 37°C for 1 hour while shaking gently. A volume of 200 µl was added to the ampicillin-containing agar plate and a bent Pasteur pipette was used to spread the mixture all over the plate. Plates were incubated at 37°C with the agar side down for 20 minutes, then inverted with the agar side up and left to grow overnight. A negative control plate containing un-transformed competent cells was included. No growth should be seen on the negative control plate as only cells carrying the ampicillin resistance-containing vector DNA should survive.

2.2.5 Large scale preparation of plasmid DNA

Single colonies were incubated in 5 ml of LB containing 50 µg/ml ampicillin and incubated at 37°C overnight with gentle shaking. One ml of the overnight culture was inoculated in 400 ml of ampicillin-containing LB in a 2 L flask and incubated overnight at 37°C with shaking. The PureYield Maxiprep System kit (Promega, USA), which makes use of a silica-membrane column filtration, was used following the manufacturer's instructions to isolate high quality plasmid DNA. Briefly, cells were pelleted by centrifuging at 5,000 x g for 10 minutes and the pellet resuspended in 12 ml of supplied Cell Resuspension Solution which contains Tris- HCl (pH7.5), EDTA and RNase A. A volume of 12 ml of supplied Cell Lysis Solution was then added to the above and mixed together by gently inverting the tube several times. This was incubated for 3 minutes at room temperature to allow for cell lysis. Neutralization Solution was added to the lysed cells and the tube inverted several times so as to completely precipitate the cellular debris. Next, the lysate was centrifuged at 7000 x g for 30 minutes at room temperature in a fixed-angle rotor to pellet the bulk of the cellular debris. The DNA-containing lysate was passed through a filtration column using a vacuum manifold, which traps the DNA on the binding membrane. The

membrane was then washed using ethanol-containing Column Wash and finally the required DNA eluted in 1 ml of Nuclease-Free water. DNA concentration was determined using the ND1000 Spectrophotometer (NanoDrop) together with the NanoDrop ND-1000 3.3 software (Coleman Technologies Inc).

2.3 Cell culture conditions and treatments

2.3.1 Medium preparation

A day before the preparation of the medium, 2 bottles of 500 mls were autoclaved together with 1 L of distilled water and 1 L beaker with a stirrer bar covered with foil paper. The powdered Dulbecco's Modified Eagle's Medium (DMEM) and $NaHCO_3$ were added to the autoclaved water while stirring until well dissolved and the pH adjusted to 7.2. The medium was immediately filter-sterilized using a 0.22 µm filter and then aliquoted into the autoclaved 500 ml bottles and stored at 4°C. Medium older than 3 weeks was re-supplemented with L-glutamine because of its instability.

2.3.2 Cell culture

Cos 7 (Green monkey epithelial kidney), HT 1080 (human fibrosarcoma) and C2C12 (mouse myoblast) cells were cultured in DMEM, supplemented with 10% heat inactivated foetal calf serum (FCS) (Gibco, UK) and 1% Penicillin-Streptomycin (P/S) antibiotics in a 37°C incubator (95% air, 5% CO_2, 65% humidity). C2C12 cells were allowed to differentiate by switching from growth medium (DMEM + 10% FBS + 1% P/S) to differentiating medium (DMEM supplemented with 2% Horse serum and 1% P/S). All cultures were routinely subjected to mycoplasma tests and only mycoplasma free cells were used in experiments.

2.3.3 Mycoplasma test

Cells grown on a coverslip in antibiotic-free media for 2-3 days were fixed in a 1:3 mixture of glacial acetic acid and methanol for 5 sec, washed briefly with water to remove the fixing solution and then air-dried at RT for 5 min. Once dried, the

DNA was stained with Hoechst 33258 (0.5 µg/ml) for 30 sec, washed briefly with water to remove excess stain and then mounted on a slide with mounting fluid at pH 5.5. The cells were viewed immediately by fluorescence microscopy under the DAPI filter. Mycoplasma negative cells stained positive with Hoechst 33258 only in the nucleus, while cells infected with mycoplasma showed staining in both the nucleus and cytoplasm.

2.3.4 Transient transfection

Transfections were performed using FuGENE HD (Roche, USA) according to the manufacturer's instructions. FuGENE is a lipid based reagent that aids delivery of DNA into mammalian cells. Cells were plated at 1.5 x 10^5 and grown to 70-80% confluence in 35 mm dishes before transfection with 1800 ng of a firefly luciferase reporter vector driven by either the wild type (WT-) *DAF* or the mutant (Mut-) *DAF* promoters. A pRL-TK vector which encodes for Renilla luciferase was included in each transfection to serve as an internal control of transfection efficiency. The cells were incubated for 48 hours and then harvested for luciferase assays. All transfections were done in duplicates.

For the C2C12 cells, differentiation was induced 6 hours post transfection by changing the medium to DMEM supplemented with 2% horse Serum and 1% P/S. The cells were then harvested and promoter activity measured after 48 and 96 hours of differentiation.

2.3.5 Luciferase assays

The luciferase assays were carried out using the Dual-Luciferase Reporter (DLR) Assay System (Promega, USA), which contains Passive Lysis Buffer used to lyse the cells, as well as buffers and substrates for both the firefly and *renilla* luciferases. Firefly and *renilla* are two different enzymes acting on different substrates to produce a luminescent reaction. DLR enables the detection of the enzymatic activity of both enzymes within a single sample.

Transfected cells were washed twice with cold PBS and then lysed with 250 µl of 1X Passive Lysis Buffer per 35 mm dish. Cells were scraped off the

plate by using the plunger of a 1 ml syringe and the protein lysates were transferred into 1.5 ml centrifuge tubes, which were incubated at -70°C for a minimum of 30 minutes.

Luciferase assays were performed according to the instructions of the manufacturer and luciferase activity was quantitated using a Luminoskan Ascent 96 well plate luminometer. Briefly, the protein lysates were thawed at room temperature, vortexed and centrifuged (Z 233 MK-2, HEMLE) at 13 000 rpm for 1 minute, and 10 µl of each sample loaded per well of a 96-well luminometer plate (DYNEX Microfluer 1). LAR II (50 µl), the substrate for firefly luciferase, was added to each well, the plate placed in the luminometer and the samples read and processed using the accompanying Ascent software. Firefly luciferase activity was stopped and renilla luciferase activity measured by adding 50 µl of Stop & Glo reagent to each well. Results obtained were normalized for transfection efficiency by dividing firefly readings by the *renilla* readings. The duplicate results were averaged and the fold activation calculated by dividing the readings obtained for the Mut-DAF by that obtained for the WT-DAF.

2.3.6 Epstein-Barr Virus (EBV) transformation of B-lymphocytes (under supervision of Ms I Baumgarten; Chemical Pathology, UCT)

Lymphoblastoid cell lines were established by transforming lymphocytes from peripheral blood of two MG patients and two healthy normal controls with the EBV as described below. Peripheral blood was spun at 1000 x g to separate the buffy coat from blood plasma and red blood cells. To remove the remaining red blood cells and plasma from the buffy coat it was further treated with Ficoll-hypaque, a high density liquid. The mixture was spun to allow the red blood cells to sink to the bottom and the plasma to move to the surface leaving the lymphocytes to form an interface layer between them. The lymphocytes were carefully taken from the interface, put into a new tube and washed twice with culture media (DMEM + 10% FCS + 1% P/S) and then incubated in 5 mls of EBV containing culture media.

The EBV culture media was prepared by culturing B95.8 cells, which serve as a source of EB virus, in a 75 cm^2 flask and allowing the media of the cells to become acidic as judged by it turning yellow. The cells were not allowed to become over confluent so as to avoid cell death. The yellow media was then collected and put in a 50 ml conical tube, then spun down at 400 x g for 10 minutes. The supernatant was removed and filtered through a 0.22 µm filter. The filtrate containing the EB virus particles without any donor cells was mixed with an equal amount of fresh medium, stored at 4°C for a maximum of 6 months and was used to transfect blood lymphocytes.

To obtain only B-lymphocyte cell lines, lymphocytes obtained as described above were cultured in phytohaemagglutinin (PHA) (Welcome Reagents Ltd, UK), to get rid of T-lymphocytes, and EBV media in 25 cm^2 flasks at 37ºC for 3 days. Cells were checked twice a week and the media changed depending on the cell growth.

2.3.7 Lipopolysaccharide (LPS) treatment of cells

Cells were plated at 5 x 10^6 in 25 cm^2 flasks containing DMEM and the next day the cells were treated with 10 µg/ml of LPS for six hours. The mRNA and protein were extracted from the treated cells and then analyzed by qRT-PCR or western blot analyses respectively. PBS was the vehicle used to dissolve LPS and therefore in all experiments, controls were included in which cells were treated with PBS instead of LPS.

2.4 Western blot analysis

2.4.1 Protein extraction

Cells were cultured in 25 cm^2 flasks in a total volume of 5 mls. Cells were spun down for 5 minutes at 400 x g and the medium removed. The cell pellets were washed twice with 1 ml of PBS and then spun in 1.5 ml microcentrifuge tubes for 4 minutes at 12,000 rpm at 4ºC. Protein extraction was performed under non reducing conditions. The lysis buffer used was prepared as shown in **Table 2.4**.

Table 2.4: Concentrations used to prepare the protein lysis buffer.

Protein lysis buffer	[Stock]	[Final]	Volume
Sodium Chloride (NaCl)	5 M	150 mM	300 µl
NP40 or Triton X-100	100%	1%	100 µl
Tris, pH 8.0	1 M	50 mM	500 µl
dH_2O			9.1 ml
Total volume			10 ml

The lysis buffer was supplemented with the appropriate protease inhibitors to maintain protein integrity. After the last washing step, cells were resuspended in lysis buffer and incubated on ice for 30 minutes and then centrifuged at 4ºC at 12,000 rpm for 20 minutes to remove cell debris. The supernatant containing the cellular protein was stored at -70ºC.

2.4.2 Protein quantification

The total protein was quantified using the BCA Protein Assay Kit (Pierce, USA) which is based on the colour producing Biuret reaction of protein on Bicichoninic Acid (BCA) substrate. The intensity of the colour produced is nearly directly proportional to the amount of protein present. Nine standards of varying Bovine Serum Albumin (BSA) concentrations (0 to 2000 µg/ml), made up in the same buffer as the samples, were used to generate a standard curve. Briefly, a one-in-six dilution of each protein sample was made up using 10 µl of sample and 50 µl of the lysis buffer. A total of 25 µl of the standards and the samples were loaded in duplicate in a 96-well plate. The BCA working reagent was prepared by combining 50 parts of BCA reagent A with 1 part of BCA reagent B (50:1, Reagent A: B) and 200 µl of this mixture was added to each protein sample. The plate was then incubated at 37ºC for 30 minutes, then quantification was

performed using the Anthos 2001 spectrophotometer at 595 nm (Anthos Labtec Instruments) and the accompanying WinRead software V.2.3. The duplicate readings of the standards were averaged together and normalized to the blank standard and these were used to construct the standard curve. The standard curve was in turn used to obtain the concentrations of the protein samples.

2.4.3 Sodium-dodecyl-sulphate polyacrylamide gel electrophoresis (SDS-PAGE)

The protein samples were separated on an 8% resolving gel (appendix A) with a 5% stacking gel (appendix A). The gels were poured in the Biorad Mini Protein 3 casting apparatus (Biorad, USA) according to the manufacturer's instruction. Different plate sizes, 1.5 mm (thick) and 0.75 mm (thin) were used according to the total volume of protein to be loaded. The BRIC 216 antibody (IBGRL, UK) recognizes the DAF protein in its non-reduced form, therefore the preparation of the loading samples was done under non-reducing conditions i.e. SDS and Dithiothreitol (DTT) were not included in the loading dye (appendix A). The PeqGold Prestained Protein marker (PeqLab Biotechnologie, Germany) (appendix B) was loaded together with the samples for calibration purposes. Protein samples were loaded onto the SDS-PAGE and the gel placed into the electrophoresis tank apparatus filled with 1 x migration buffer (appendix A). Electrophoreses occurred at 100 Volts for approximately 90 minutes which gave a good separation of the proteins.

2.4.4 Protein transfer

Following separation of proteins on the gel, the protein was electrophoretically transferred onto a Hybond-ECL Nitrocellulose membrane (Amersham Biosciences, Germany), that was cut to the required size and trimmed at the left hand corner to identify the order in which samples were loaded. The membrane was carefully labeled with the date, amount of protein and the name of the cell lines used and then soaked in 1 x transfer buffer (appendix A). The gel and the membrane were sandwiched between wet sponge and wet Whatman filter paper

(Schleicher & Schuell, Germany) in the following order: sponge/filter paper/gel/membrane/filter paper/sponge. All were securely clamped together and bubbles were avoided between the gel and the membrane. The whole assembling was performed in the transfer buffer to avoid the drying of the membrane. The sandwich was submerged in the transfer buffer and electrophoresis was applied at 100 Volts for 1 hour or 1 hour 30 minutes according to the thickness of the gel.

2.4.5 Western blot detection

After the transfer, the membrane was rinsed twice in 1 x PBS/0.1% Tween (appendix A) and then blocked in 5% milk in 1 x PBS/0.1% Tween for 1 hour at room temperature with a bit of shaking. The primary antibodies were diluted as follows: BRIC 216 DAF monoclonal antibody was diluted in milk at 1:100 dilution, and the p38 rabbit polyclonal antibody (Cell Signaling Technology Inc., USA) was diluted in 1 x PBS/0.1% Tween at 1:5000 dilution. The membranes were incubated with the primary antibodies overnight at 4ºC and then washed with 1 x PBS/0.1% Tween two times 10 minutes and two times five minutes. After the washes the membranes were incubated for 1 hour at room temperature with gentle shaking with peroxidase conjugated anti-mouse and anti-rabbit secondary antibodies for DAF and p38 proteins, respectively. The blots were washed as before i.e. twice for 10 minutes and twice for five minutes before detection with the SuperSignal® West Pico Chemiluminescent Substrate kit (Pierce Biotechnology, USA). A total of 1 ml of the substrates A and B detection reagents (ratio 1:1) were added to a blot for 1 minute before the blot was sandwiched between acetate sheets in a cassette. The blot was exposed to X-ray film for varying times and the film processed by immersing it in developer for five minutes, then washing in water and fixing for five minutes. The films were then washed thoroughly with water and left to air-dry.

2.4.6 Stripping nitrocellulose membranes

The membranes were immersed in pre-heated (at 55ºC) stripping buffer (appendix A) for 30 minutes, and then washed two times 10 minutes in 1 x PBS/0.1% Tween, after which standard western blots procedures followed.

2.5 *DAF* mRNA expression analysis by quantitative real-time PCR (qRT-PCR)

Currently, qRT-PCR is the most precise method to measure and quantify mRNA levels. Quantitative RT-PCR is a PCR process in which an amplification product can be detected and measured simultaneously during each PCR cycle. This is achieved by using SYBR Green I, which is a fluorescent dye that is incorporated into the growing double stranded cDNA and emits a fluorescent signal on binding. The intensity of the fluorescence can then be correlated to the amount of PCR product. The reaction is characterized by a crossing point (C_T), also known as the threshold cycle, which is the point where the target amplification is first detected. At this point the fluorescence intensity is greater than the background.

The qRT-PCR reactions are carried out in glass capillaries that are placed in a thermocycler, Lightcycler machine (Roche, Germany), which controls the temperature required at each cycle of PCR, then exposed to excitation energy and the resulting fluorescence is measured by a photodetector. The cycling conditions are similar to those used in conventional PCR, however, in qRT-PCR there is inclusion of a melting curve step. This is an important step for reactions that make use of SYBR Green based kits, as SYBR Green can detect any double-stranded DNA including primer dimmers, contaminating DNA and PCR products of misannealed primer. Therefore, the melting curve analyses are carried out to ensure product specificity.

2.5.1 RNA extraction from whole blood

Quantification of messenger RNA (mRNA) levels in peripheral blood is complicated by the fact that mRNA is very unstable. It has been shown that unpreserved whole blood is readily degradable and that the copy numbers of

individual mRNA species can change more than a 1000-fold during storage or transport at room temperature (Rainen et al., 2002). To avoid rapid degradation, the collection and handling of the blood samples should be carried out carefully. Several methods of blood collection have been employed that use anticoagulants like EDTA, heparin and citrate salts. These reagents prevent clotting but are unable to maintain the in-vivo gene transcript copy numbers. The collection of the whole blood in the above mentioned anticoagulants has been shown to be unstable over time (Rainen et al., 2002). For this reason we used the PAXgene™ Blood RNA System (PreAnalytiX, QIAGEN /BD Company, USA) that includes the PAXgene RNA collection tubes which have been shown to reduce RNA degradation in whole blood samples. The tubes contain a reagent that immediately stabilizes RNA by protecting its degradation by RNases and also by minimizing ex vivo changes in gene expression (Rainen et al., 2002).

According to the manufacturer's instructions, 10 ml of venous blood was collected into PAXgene tubes and kept at room temperature for 2 hours to allow for complete lysis of blood cells. The tubes were then stored at 4°C or -20°C, depending on the time lapse before RNA extraction. If RNA was to be extracted from the blood within 5 days then blood was stored at 4°C but if RNA extraction was to be done within 2 weeks to 6 months, blood was stored at -20°C. Total RNA was extracted from whole blood using the PAXgene Blood RNA kit. Briefly, the nucleic acids were pelleted by centrifuging the lysed blood in the PAXgene tubes. Proteins were digested by addition of optimized buffers together with proteinase K. RNA-containing lysate was filtered through a PAXgene Shredder spin column and ethanol added to allow selective binding of RNA in the filtrate while spinning contaminants through the PAXgene RNA spin column. DNase I was included in subsequent washes to remove the traces of bound DNA. The purified RNA was finally eluted in elution buffer and heat denatured.

2.5.2 RNA extraction from lymphoblastoid cell lines

Total RNA extraction from Epstein-Barr virus (EBV) transformed lymphoblastoid cell line (LCL) cultures was performed using the RNeasy Plus Mini Kit (QIAGEN,

USA). Diethyl pyrocarbonate (DEPC) treated microfuge tubes and pipette tips (Appendix A) were used to minimize RNA degradation during the extraction process as DEPC destroys RNases. Cells were harvested by centrifugation and then homogenized in a denaturing guanidine-isothiocyanate-containing buffer. Effective removal of genomic DNA (gDNA) is facilitated by passing the homogenate through a specially designed genomic DNA Eliminator spin column. This is important as the presence of gDNA can result in false positives if amplified during the reverse transcription step. The RNA in the flow-though was allowed to bind to the membrane of the RNeasy spin column by addition of ethanol prior to centrifugation. Purified RNA could then be obtained by elution with RNase free water.

2.5.3 Measuring RNA concentration and integrity

The concentration and purity of purified RNA was determined using the NanoDrop as described for DNA in section 2.1.3. RNA integrity was additionally assessed by electrophoresis on a 1% agarose gel and observing the separation between 28S and 18S bands by visual assessment under the UV transilluminator. This is important because the success of the reverse transcription process depends on the integrity and purity of the starting RNA

2.5.4 Reverse transcription

RNA is very easily degraded by RNases that are always present in the environment; therefore, the RNA is usually converted to complimentary DNA (cDNA), which is more stable and more convenient to work with. cDNA is a double-stranded DNA synthesized from RNA during the reverse transcription process using the reverse transcriptase (RT) enzyme. mRNA was transcribed into cDNA by using the Improm-II Reverse Transcription System (Promega, USA) following the manufacturer's instructions. All microfuge tubes and pipette tips were DEPC treated before use. Briefly, either 500 ng or 1 µg of RNA was combined with 1 µl of Oligo $(dT)_{15}$ primer in a total volume of 5 µl, and then heat denatured at 70°C. The reverse transcription mix (**Table 2.5)** was then added.

The mixture was incubated for 5 minutes at 25°C in a controlled-temperature heating block for the annealing process to take place and the cDNA strands allowed to extend at 42°C for an hour. The Reverse Transcriptase was then inactivated at 70°C for 15 minutes and the cDNA stored at -20°C. A negative (No-Template) control was prepared by replacing RNA template with nuclease free water. It was deemed unnecessary to include a negative (no RT) control in which no reverse transcriptase was added, as the PCR primers were designed to eliminate the possibility of amplifying genomic DNA and DNase I was included in the RNA extraction process.

Table 2.5: Components of the Improm-II Reverse Transcription System used in the reaction

Reagent	**Stock volume**	**Final concentration**
Reagent buffer	4 µl	1 x
$MgCl_2$	2.4 µl	3 mM
dNTP mix	1 µl	0.5 mM each dNTP
Recombinant RNasin Ribonuclease Inhibitor	0.5 µl	20 units
Reverse Transcriptase	1 µl	
Nuclease Free Water	6.1 µl	
Total volume	**15 µl**	

2.5.5 Quantitative Real-time PCR (qRT-PCR)

The Sensimix Lite kit (Quantace, UK) was used to quantify the mRNA expression levels of the target gene gDAF and the house-keeping genes GUS and GAPDH following the manufacturer's instructions. Briefly, reagents were mixed in glass capillaries to a final volume of 10 or 20 µl as shown in **Table 2.6**. The procedure was performed in the Lightcycler machine and the levels of fluorescence were quantified using the accompanying Light Cyler Software Version 3 (Roche, Germany). Cycling conditions were generally similar for the gDAF and the house

keeping genes but differed in the holding times in the cycling step as shown in **Tables 2.7** and **2.8**. Similarly to conventional PCR, the several parameters altered to achieve optimal conditions. After the amplification process, the PCR products were run on a 3% agarose gel to ensure that the right sized products were obtained.

Table 2.6: Summary of optimized real time PCR parameters used for amplification of gDAF, GUS, GAPDH genes.

Reagent	gDAF	GUS	GAPDH
5 x SensiMix Lite (dNTPs, 15 mM $MgCl_2$, stabilizers)	4 µl	2 µl	2 µl
Enzyme mix (Taq DNA Polymerase)	1.5 µl	0.75 µl	0.75 µl
50 x SYBR green	0.4 µl	0.2 µl	0.2 µl
Primers (10 pmol)	Fwd: 0.4 µl Rev: 0.4 µl	1.5 µl of combined fwd and rev primers	0.6 µl of combined fwd and rev primers
Sterile water	12.3 µl	4.55 µl	5.45 µl
cDNA	1 µl	1 µl	1 µl
Total volume	20 µl	10 µl	10 µl

Table 2.7: Summary of real time PCR optimal cyclic conditions used for the gDAF.

	Cycle number	Target °C	Holding time (mins)	Ramp/Slope (°C/sec)
Activation	1	95	10:00	0
Cycling	35			
Denaturation		95	00:15	20
Annealing		55	00:30	20
Extension		72	00:30	20
Melting	1			
Denaturation		95	00:00	20
Annealing		65	00:15	20
Melting		95	00:00	0.1
Cooling	1	40	00:30	20

Table 2.8: Summary of RT-PCR optimal cyclic conditions used for the GUS and GAPDH.

	Cycle number	Target °C	Holding time (mins)	Ramp/Slope (°C/sec)
Activation	1	95	10:00	0
Cycling	35			
Denaturation		95	00:03	20
Annealing		55	00:05	20
Extension		72	00:03	20

2.5.6 Quantification of mRNA and establishing the standard curves

There are two types of RT-PCR quantification, absolute quantification and relative quantification. The absolute quantification allows the expression level of the target gene to be given as an absolute copy number. Absolute quantification employs a standard curve that is generated by the use of serially diluted standards of known concentrations. Relative quantification is when the level of gene expression is calculated by a comparative crossing point method in which changes in gene expression are calculated as relative fold difference between

the sample and the control. House-keeping genes are genes that are usually expressed to effect basal cellular function and are used as endogenous reference genes whose expression level should not differ from sample to sample or between patients and controls (Eisenberg and Levanon, 2003). The house-keeping gene is used as a reference and can indicate variability in the processes leading to qRT-PCR, such as RNA extraction process and reverse transcription process.

The amplification efficiencies for the target gene and the house-keeping gene should be comparable for one to carry out relative quantification using the comparative method. If the efficiencies of the two genes are not comparable, an external standard has to be employed (Giulietti et al., 2001). Amplification efficiency is the rate at which the PCR products are increasing exponentially. The efficiency of RT-PCR is shown by the value of the slope of the standard curve. A reaction is said to be 100% efficient when it has a slope of -3.322 and any value less than this is an indication that the PCR is less than 100% efficient. If the amplification efficiencies of the target gene and the house-keeping gene are not equal, the quantity of each sample is first calculated using the standard curve and then it is expressed as a ratio of the amount of the house-keeping gene concentration calculated from the standard curve.

To construct a standard curve, serial dilutions from the cDNA of a normal healthy control (BN) sample were prepared according to the given protocol (see Appendix C). The cDNA was amplified in excess for each set of primers, Gspec (for gDAF gene), GUS and GAPDH, by setting up five PCR reactions of 20 µl each on the Lightcycler machine and a small volume of the PCR product run on a 2% agarose gel to check that the PCR product was of the right size. The amplification reactions were then transferred from the lightcycler capillaries into microfuge tubes and cleaned up using the Wizard SV Gel and PCR Clean-up System (Promega, USA) as per manufacturer's instruction. The concentration and the integrity of the purified PCR product was measured using the NanoDrop spectrophotometer as described before.

A dilution series from 10^7 down to 10^3 was prepared for gDAF, GUS and GAPDH purified PCR products, in order to be able to construct a standard curve for each gene. RT-PCR was performed in triplicate for all the dilutions and standard curves were constructed on the Roche Lightcycler by plotting the C_T values on the y-axis against the log of the initial template concentration. There is a linear relationship between the C_T and the initial amount of the total RNA or cDNA, and this allows for the calculation of the concentration of the unknown samples. The standard curve was only constructed once for each gene. Therefore it is important to include one of the standard curve serial dilutions in each subsequent run in order to normalize against the standard curve to correct for inter-assay variability. The qRT-PCR data was analyzed by relative quantification, using both the standard curve and the $2^{-\Delta\Delta Ct}$ methods (presented by PE Applied Biosystems, Perkin Elmer, CA).

2.6 Transcription factor binding site (TFBS) analysis

We performed a direct matching of the known TFBSs contained in the TRANSFAC Professional database v.11.2. (Matys et al., 2006). This has been done with the Patch™ program of the Transfac suite (Matys et al., 2006). We used matching of motifs with length of 7 bp and with no mismatch between the template motif and the matched sequence. We considered that the motif is affected by the SNP if it includes the SNP nucleotide. Our results indicate that a Sp1 binding site in genomic sequence (C nucleotide version) has been lost when G nucleotide replaced C nucleotide. The new putative TFBS obtained was that of a NF-$_K$B binding site.

CHAPTER 3: RESULTS

All patients used in this study had been diagnosed with MG by Prof Heckmann as described (Heckmann et al., 2007), and had attended more than two follow up visits at the University of Cape Town Myasthenia clinic, located at Groote Schuur Hospital. In a previous study, Heckmann et al., 2007 observed that more MG patients of African ancestry (Blacks and M/A) were developing a treatment-resistant severe extra-ocular muscle (EOM) MG phenotype compared to the White patients. The EOMs have been shown to express less complement regulatory proteins (CRPs) than other tissues (Kaminski et al., 2004; Conti-Fine et al., 2006) and are thus more susceptible to diseases associated with complement damage such as MG. Of the known CRPs, DAF has been shown to provide the substantial protection for the eye tissues (Lass et al., 1990) from complement injury. A lack of DAF has also been shown to increase susceptibility to complement injury in mice as described in the introduction (Lin et al., 2002).

3.1 Two SNPs were found in the 5` upstream region of the *DAF* gene

To determine whether the severe EOM MG phenotype is due to reduced DAF expression, the first aim of this study was to screen for base changes in the 5` upstream regulatory and selected coding regions of the DAF gene. The minimal promoter region of the *DAF* gene was PCR-amplified from DNA obtained from 136 MG individuals and 167 healthy racially matched controls. The PCR primers were designed for the amplification of approximately 500 bp upstream of the ATG start codon of the DAF gene. Agarose gel electrophoresis of PCR products revealed a band of the expected size (**Figure 3.1**) for each sample tested and no band was observed in the negative (no template) control. The absence of non-specific bands in the lanes rendered the PCR sample suitable for direct sequencing without the need for further cleanup processes.

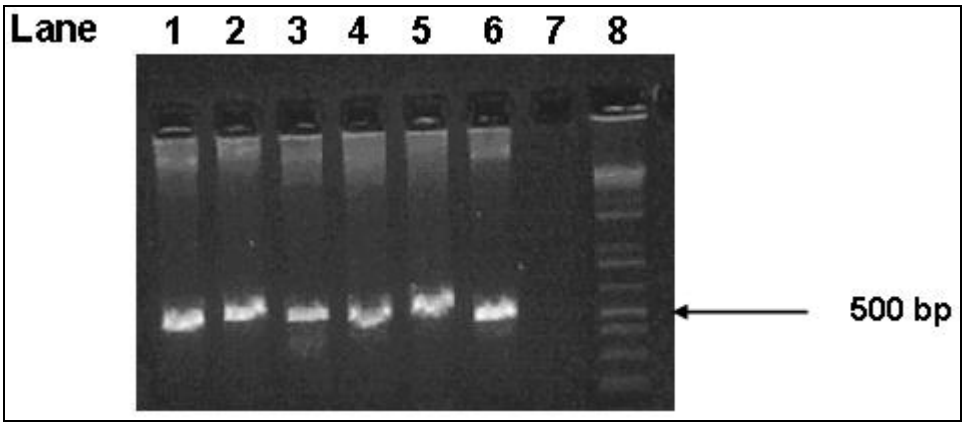

Figure 3.1: Bands of approximately 500 bp of the DAF promoter were PCR-amplified as shown by the photograph of a 2% agarose gel. Lane 1-6 = DNA samples; 7 = water blank; 8 = Molecular Weight marker (GelPilot 100 bp Plus Ladder).

Sequencing was generally performed in one direction using the sense primer and where necessary in both directions. The PCR products were cycle sequenced and then ethanol precipitated before they were electrophoresed and analyzed on the ABI Prism 3100 system. The analysis program provides electropherograms showing peaks of different colours for the four bases (**Figure 3.2 and 3.3**). Whenever the program reads a peak as N it is because of the uncertainty of the base at that position. Insertions, deletions or base changes within the sequence were easily detected by comparing to the consensus DAF sequence as obtained from Genebank RefSeq-file NM_000574. These changes may cause a shift in one strand in relation to the other in the electropherogram making it difficult to read beyond the base change. Two SNPs were found to be of interest to this study with regard to MG. These were the c.-244_-243insA, an adenine insert between nucleotides -244 and -243, and the c.-198C>G, a cytosine to guanine change at position -198 from the transcription start site.

The electropherograms for (**A**) the normal sequence with CC alleles, (**B**) the heterozygotes with CG alleles, and (**C**) the GG homozygous sequence are shown in **Figure 3.3**. A single peak (shown by the arrow in **Figure 3.3A** and **C**) shows that both alleles of the gene have the same base at that point, indicating homozygosity. In the case of heterozygosity (**Figure 3.3B**), two peaks of similar heights which are superimposed on each other and have reduced height compared to a single peak, are detected (shown by the arrow in **Figure 3.3B**).

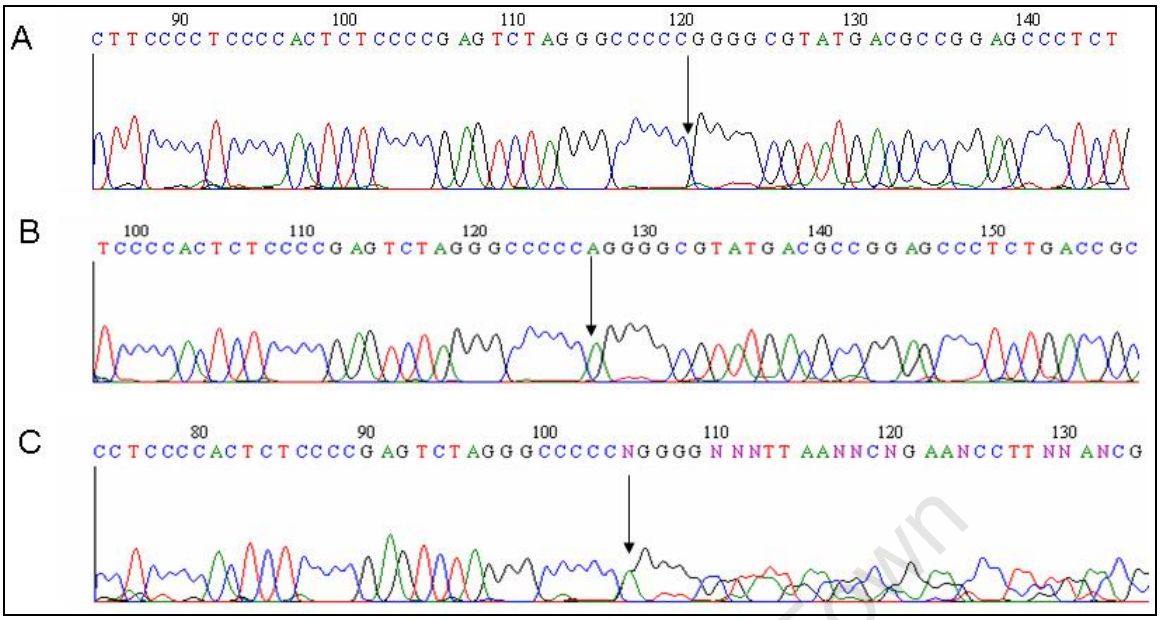

Figure 3.2: Sequencing electropherograms showing the position where the c.-244_-243insA occurred. Diagram **A**) shows the normal sequence with no insert. **B**) shows the sequence with a homozygous A insert and **C**) shows a sequence with a heterozygous A insert and the subsequent shift of one strand to another.

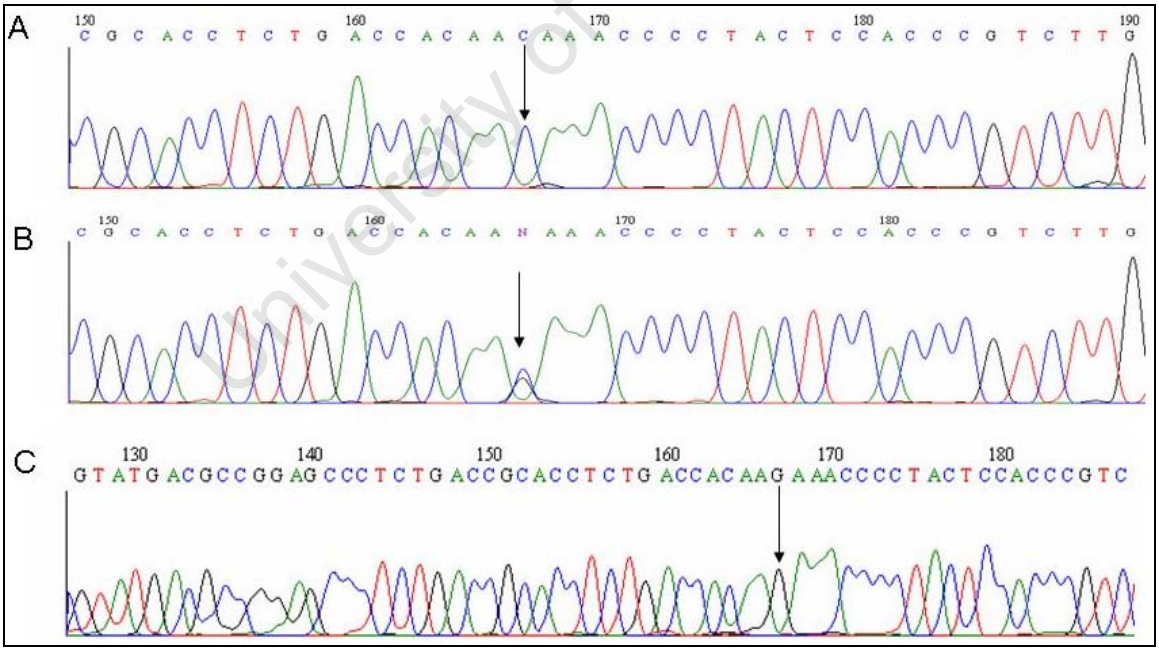

Figure 3.3: Sequencing electropherograms of part of the DAF promoter region showing **A**) normal sequence and **B**) the c.-198C>G heterozygous SNP indicated by the arrow and **C**) showing homozygosity for the G allele at position -198.

3.2 The c.-198C>G SNP is more prevalent in the African genetic ancestry individuals and is more associated with the severe EOM MG phenotype.

The c.-244_-243insA was observed in 28 out of 136 of the MG patients and 50 out of 167. Of these changes, six patients and nine controls were homozygous and 22 patients and 41 controls were heterozygous for the variant (**Table 3.1**). In all of the heterozygotes the reading sequence beyond the SNP insertion point became unreadable and the PCR products had to be sequenced in the reverse direction to check for sequence changes in the region beyond the A insert (**Figure 3.2C**). No additional changes to the sequence of the minimal promoter were observed in individuals carrying the A insert. The c.-244_-243insA was observed to be more prevalent in the controls of African-ancestry (Black and M/A) (49 of 132) compared to the White controls (1 of 35) (**Table 3.1**). A similar trend was observed among the MG patients with 27 of 103 of those of African genetic ancestry with the A insert compared to only 1 of 34 of the White MG patients. The c.-244_-243insA SNP allele frequencies did not appear to differ between the MG patients and the control individuals and therefore was not investigated further.

Table 3.1: Comparison of c.-244_-243insA allelic frequency and (%) within the MG patients and controls

Subpopulation	Wild type(%) -/-	Heterozygous(%) A/-	Homozygous(%) A/A	Total
MG patients				**136**
Black	19(63.3)	10(33.3)	1(3.3)	30
Mixed-ancestry	56(77.8)	11(15.3)	5(2.5)	72
White	33(97.1)	1(2.9)	0	34
Controls				**167**
Black	25(52.1)	20(41.7)	3(6.3)	48
Mixed-ancestry	58(69.1)	20(23.8)	6(7.1)	84
White	34(97.1)	1(2.9)	0	35

Overall, the c.-198C>G SNP was identified in eight out of 136 MG patients and six out of 167 controls (**Table 3.2**). There was only one homozygote for the variant and the remaining patients were all heterozygous. All of the c.-198C>G SNPs were detected in individuals of African ancestry (Black and M/A) and was absent in both the White MG patients and controls. No additional base changes were observed in the minimal promoter in individuals carrying the c.-198C>G SNP.

Table 3.2: Comparison of the allelic frequency in individuals (%) with the c.-198C>G in the MG patients and controls

Subpopulation	Wild type (%) CC	Heterozygous (%) CG	Homozygous (%) GG	Total
MG patients				**136**
Black	26 (86.7)	4 (13.3)	0	30
Mixed-ancestry	68 (94.4)	3 (4.2)	1 (1.4)	72
White	34 (100)	0	0	34
Controls				**167**
Black	46 (95.8)	2 (4.2)	0	48
Mixed-ancestry	80 (95.2)	4 (4.8)	0	84
White	35 (100)	0	0	35

The allelic frequencies and odds ratio of the c.-198C>G in association with the EOM phenotype are shown in (**Table 3.3**). Overall, the c.-198C>G SNP did not show significant association with the MG patients, but was found to be significantly more associated with the African ancestry MG patients having the severe EOM phenotype (p = 0.009). The MG subjects belonging to the Black subpopulation were more likely to develop paresis of at least one EOM if they have the c.-198C>G promoter SNP as shown by the odds ratio of 12.9 (p = 0.006). The Black MG patients with the c.-198C>G SNP also had increased likelihood of developing pareses of at least 5 EOMs (p <0.01). Similarly, in the M/A patients the SNP was significantly associated with the developing of one or more EOM dysfunction (p = 0.022) but not with the developing five or more EOM paresis (p-value = 0.27). However, when the findings for the patients of African genetic-ancestry (Black and M/A) were combined, the likelihood of developing EOM with at least five or more dysfunctions was significantly increased in the patients with the SNP (p-value = 0.009)**.** None of the White MG subjects had the c.-198C>G.

Table 3.3: Association of the c.-198C>G SNP with treatment-resistant EOM involvement in South African MG subpopulation

			G allele			Genotype		CG+GG/CC	
Subpopulation	Phenotype	N (%)	Freq.	Odds ratio (95% CI)	P-value	CC	CG/GG	Odds Ratio (95% CI)	P-value
Black	EOM-N	21 (70)	0			1.0	0		
	EOM≥1	9 (30)	0.222	**12.9** (2.1-108.7)	**0.006**	0.555	0.444	**18.4** (2.7-127.0)	**0.004**
	EOM≥5	6 (20)	0.250	**15.7** (2.3-106.4)	**<0.01**	0.500	0.500	**23.0** (2.7-194.8)	**0.008**
	C	48	0.021			0.958	0.042		
M/A	EOM-N	53 (74)	0.009			0.981	0.019		
	EOM≥1	18 (25)	0.133	**6.2 (1.3-29.1)**	**0.022**	0.833	0.167	4.0 (0.8-19.7)	0.07
	EOM≥5	15 (21)	0.067	2.9 (0.4-17.2)	0.27	0.867	0.133	3.1 (0.5-18.5)	0.275
	C	84	0.024			0.952	0.048		
African-ancestry	EOM-N	74 (73)	0.006			0.987	0.013		
	EOM≥1	27 (26)	0.148	**8.6** (2.8-26.1)	**0.0003**	0.740	0.259	**7.4** (2.2-24.1)	**0.002**
	EOM≥5	21 (21)	0.238	**5.8** (1.7-20.0)	**0.01**	0.762	0.238	**6.6** (1.8-24.1)	**0.009**
	C	132	0.023				0.045		
White #	EOM-N	28 (82)	0			1	0		
	EOM≥1	5 (15)	0			1	0		
	EOM≥5	2 (6)	0			1	0		
	C	35	0			1	0		
SNP-NCBI**	Af-Amer.	23	0.022			0.978	0.043		
	European	23	0			1	0		

EOM= Extraocular muscle; EOM-N= normal eye movement; EOM≥1 = a least one of the 12 EOM's is dysfunctional; EOM≥5 = a least 5 out of 12 dysfunctional EOM's; C = racially matched controls; **ss32475790; # One individual with thyroid eye disease excluded from the analysis; Odds ratios were calculated relative to the normal controls; The exact p-values are 2-tailed; 95% CI = 95% confidence intervals; M/A = Mixed Ancestry; African-ancestry = Black + M/A.

The DNA samples from 50 MG individuals were screened for base changes in exons 3, 4 and 5 which encode critical components of the classical complement pathway. No genetic variants were observed in these three exons or in their intron-exon splice junctions and for this reason comparative studies with normal healthy controls were not deemed necessary. Eleven MG patients representing a spectrum of clinical phenotypes were screened for mutations in the region of exons 7, 8, 9 and 14 which encode for the GPI membrane anchorage for the DAF gene. Similarly, no sequence variations were observed in these exons.

3.3 The c.-198C>G affects basal DAF promoter activity

Once it was established that the c.-198C>G was significantly associated with the severe EOM MG phenotype, we investigated its effect on the DAF promoter activity using site directed mutagenesis and luciferase reporter assays. The guanine residue at position -198 within the DAF promoter, already cloned into a pGL3 luciferase vector, was mutated to cytosine by site-directed mutagenesis (generated by Dr H. Teng) and is referred to as Mut-DAF promoter throughout this thesis.

To determine the suitable amount of plasmid DNA to use for transient transfections, various concentrations (450 ng, 900 ng and 1800 ng) of the firefly reporter driven by either the wild type WT- or Mut-DAF promoter constructs were transfected into the HT 1080 cells and luciferase activity was measured. This cell line was used due to its ability to easily take up foreign DNA. The TK-renilla construct was included in all experiments as an internal control for measuring transfection efficiency. The results of one transfection experiment, which is representative of two independent experiments performed each time in duplicate, are shown in **Figure 3.4**. While very little difference in luciferase activity was observed between the WT- and the Mut-DAF promoter activity in the cells transfected with 450 ng and 900 ng of DNA, cells transfected with 1800 ng of DNA showed that the Mut-DAF promoter had approximately 2-fold more activity

than the WT-DAF promoter. Based on these results, 1800 ng of DNA was used in all future transfection experiments.

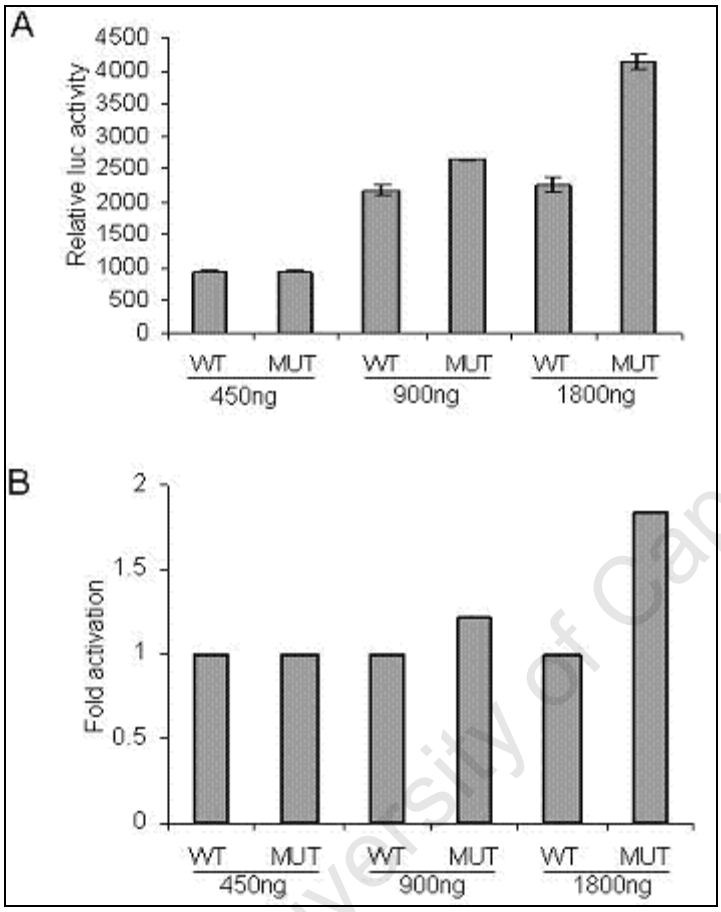

Figure 3.4: Dose curve to determine the amount of plasmid DNA to be used in transient transfections. HT 1080 cells were transfected with 450 ng, 900 ng or 1800 ng of either the WT- and Mut-DAF promoter reporter constructs. After a 30 hour transfection period, cells were lysed and data was normalized against TK Renilla to determine promoter activity (**A**). A significant difference between WT- and Mut-DAF promoters was observed using 1800 ng of DNA as shown by the fold activation graph in (**B**). The results shown are representative of two independent experiments performed in duplicate.

To confirm that the effect of the c.-198C>G SNP on DAF promoter activity observed above was not cell type dependent, COS-7 cells were included in the next set of experiments which were carried out as the previous experiment with

1800 ng of either WT- or Mut-DAF. **Figure 3.5 A** and **C** show that the relative luciferase activities in both cell lines were higher in the cells transfected with the Mut-DAF compared to the WT-DAF. On average, a 2-fold increase in the Mut-DAF promoter activity was observed in comparison to the WT-DAF in both cell lines (**Figure 3.5 B and D**). These results confirmed that the c.-198C>G SNP resulted in an increase in DAF promoter activity and that this effect was independent of the cell type used.

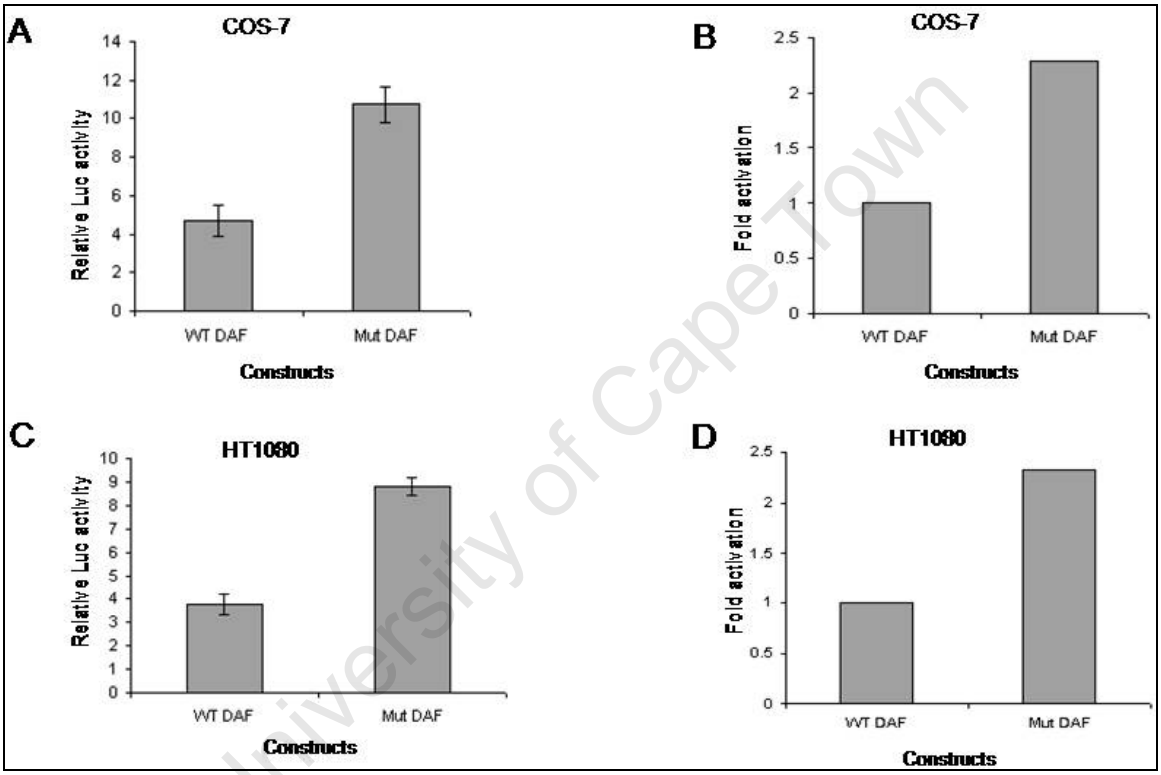

Figure 3.5: Effect of c.-198 C>G SNP on DAF promoter in COS 7 (**A** and **B**) and HT1080 (**C** and **D**) cells. The cells were transfected at approximately 80% confluency with 1800 ng of WT- or Mut-DAF promoter constructs. TK-Renilla luciferase was used as an internal control for transfection efficiency. The cells were lysed after 30 hours of transfection and luciferase activity measured. The results were normalized against the TK-Renilla activity and the relative luciferase activity represented in bar graphs **A** (COS 7 cells) and **C** (HT1080 cells). **B** and **D** show the ~ 2-fold increased activation observed in the cells transfected with the Mut- compared to the WT-DAF of COS 7 and HT1080 cells, respectively. The results shown are representative of 3 independent experiments that were performed in duplicate. The error bars indicate standard error.

The next experiment was conducted to determine whether the effect of the c.-198C>G SNP seen above could be repeated in muscle cells, which is more representative of the tissue involved in MG patients. This was investigated by transiently transfecting the undifferentiated muscle cell line C2C12 as above with 1800 ng of either the WT- or Mut-DAF. In these experiments, some C2C12 cell plates were harvested after 30 hours of transfection and other cell plates were allowed to differentiate by changing the growth medium to differentiation medium supplemented with 2% Horse serum and left for another 48 hours. These will henceforth be referred to as undifferentiated and 48-hour differentiated C2C12 cells, respectively. **Figure 3.6** shows that after 48 hours in differentiation medium the spindle-shaped cells had started to fuse and become more elongated to form thin muscle fibres. The results of one transfection experiment, which is representative of three independent experiments done each time in duplicate, are shown in **Figure 3.7**. As can be seen, the c.-198C>G SNP led to an approximately 2-fold increase in the activity of the Mut-DAF promoter in both undifferentiated and 48-hour differentiated C2C12 cells thus confirming the results shown in **Figure 3.5**. Cells in some plates were left in differentiation medium for a period up to 10 days to determine the effect of the c.-198C>G SNP on promoter activity during prolonged differentiation period. The cells were lysed and luciferase activity determined. Three independent experiments were performed each time in duplicate. Unfortunately, the results showed negligible *renilla* luciferase activity indicating poor transfection efficiency and there was no significant difference between the WT- and Mut-DAF (Data not shown).

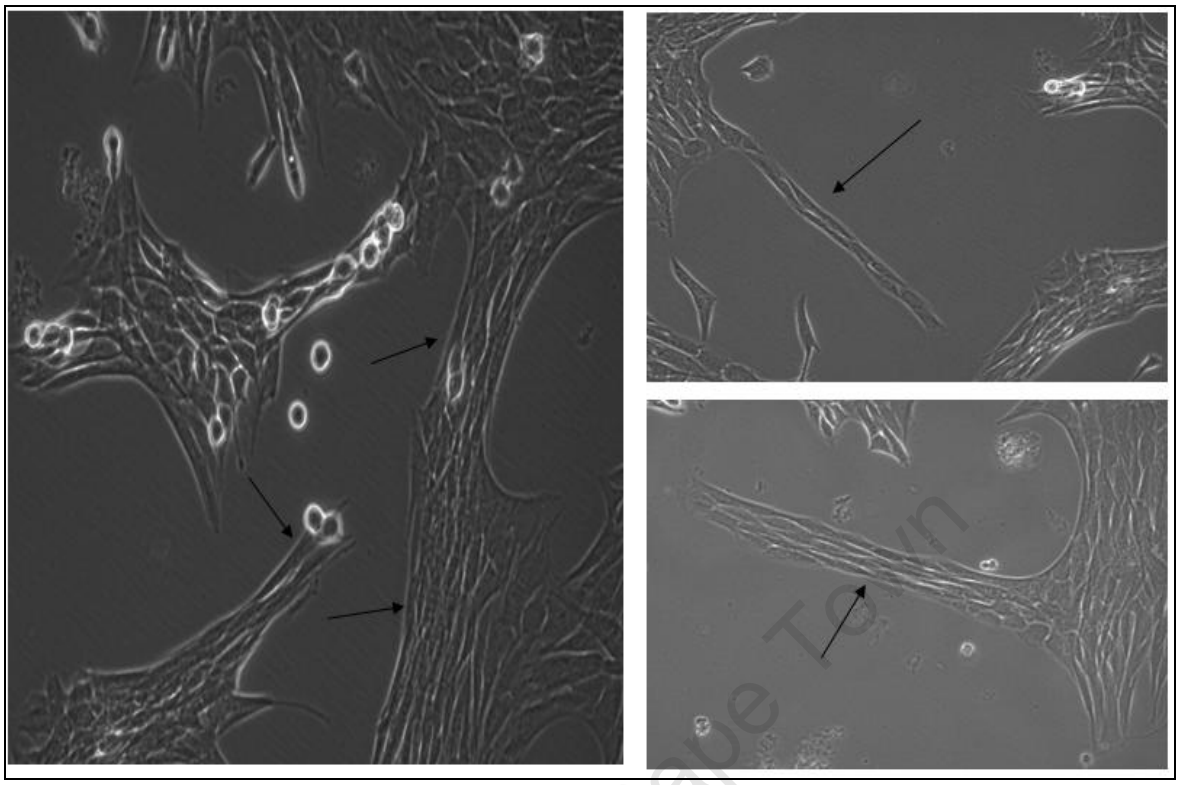

Figure 3.6: 48-hour differentiated C2C12 cells. C2C12 cells were allowed to differentiate by changing the growth medium (DMEM + 10% FCS + 1% P/S) to differentiation medium (DMEM + 2% Horse Serum + 1% P/S) and incubating them at 37ºC for 48 hours. After 48 hours the spindle-shaped myoblast-like cells started to fuse together and form the long thin muscle fibres (shown by the arrows).

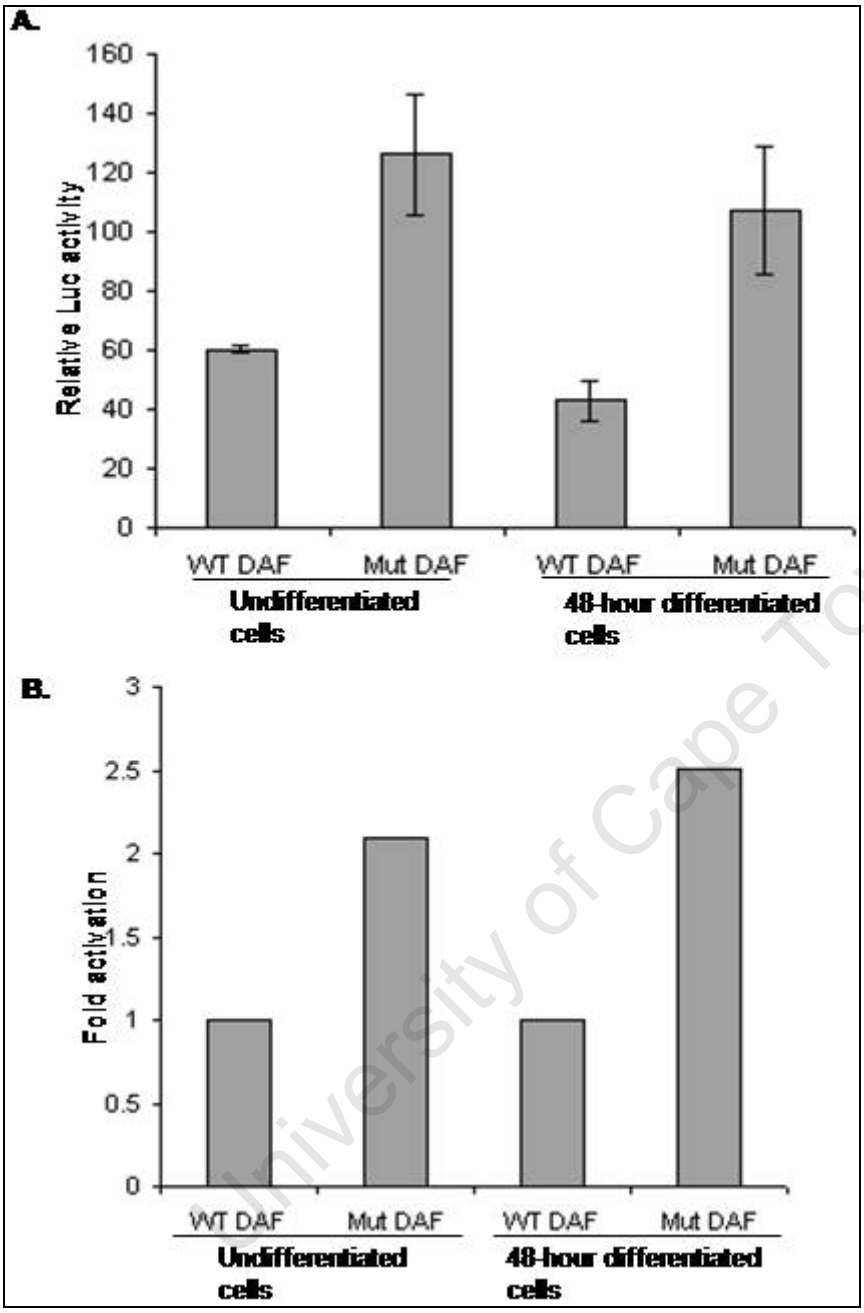

Figure 3.7: Luciferase activity in C2C12 (Mouse myoblasts) cells. Cells were transfected with 1800 ng of either the WT- or the Mut-DAF constructs and harvested after 30 hours of transfection. For differentiation, the growth medium was substituted with differentiation medium containing 2% Horse serum and allowed to differentiate for 48 hours. Cells were lysed and the data normalized to TK *renilla* to obtain luciferase activity (**A**). There was ~ a 2-fold increase in the Mut-DAF compared to the WT-DAF in both the undifferentiated and the 48-hour differentiated C2C12 cells (**B**). The results shown are representative of 3 independent experiments that were performed in duplicate. The error bars indicate standard error.

3.4 The c.-198C>G does not appear to have any effect on endogenous *DAF* mRNA expression levels in the human lymphocytes

Having shown that the c.-198C>G led to increased promoter activity in the Mut-DAF, the effect of the c.-198C>G SNP on DAF mRNA levels in MG patients was next investigated. Total RNA was extracted from blood lymphocytes contributed by eleven MG patients attending the MG clinic. These patients had varying clinical characteristics as shown in **Table 3.4**.

Table 3.4: The clinical characteristics of the MG patients used for peripheral blood lymphocyte *DAF* mRNA expression

Patients	Gender	Promoter genotype	Number of EOMs affected	Lymphoblastoid cell lines obtained
Patient 1	F	G/G	0	-
Patient 2	F	G/G	≥5	-
Patient 3	F	G/G	0	-
Patient 4	F	G/G	0	✓
Patient 5	M	C/G	≥5	✓
Patient 6	F	G/G	≥5	-
Patient 7	F	G/G	≥5	-
Patient 8	F	G/G	0	-
Patient 9	M	G/G	≥5	-
Patient 10	M	C/G	≥5	✓
Patient 11	M	C/G	≥5	✓

* Patient 4 had severe generalised refractory MG without ocular involvement.

Whole blood was also collected from 6 controls for RNA extraction. The extracted RNA was reverse transcribed into cDNA and *DAF* mRNA was quantified using quantitative real-time PCR (qRT-PCR) with primers specific to the *gDAF* isoform. *DAF* relative expression levels were normalized against the house-keeping genes, GUS and GAPDH.

Figure 3.8 shows the result of a typical qRT-PCR experiment. During the PCR amplification, the accumulation of fluorescent emission at each reaction cycle is plotted on the PCR amplification curve for each sample. The amplification curve can be divided into three main phases, the linear ground phase, the exponential phase and the plateau phase (as outlined in Critical factors for successful Real-time PCR handbook). The linear ground phase is a reflection of no detectable increase in fluorescence due to amplification products. As the reaction moves into the exponential phase, there is an increase in the product and finally the reaction enters the plateau phase where no additional product is detected. **Figure 3.8B** shows the melting curves for these reactions showing a single peak at a temperature of about 85ºC. The single peak indicates the presence of a single product and the absence of primer-dimer contamination. Aliquots of the qRT-PCR reactions were run on 2% agarose gels to confirm that the peak on the melting curve was generated from a PCR product of the expected size (**Figure 3.9**). The correct product sizes were: gDAF (322 bp), GAPDH (119 bp) and GUS B (96 bp).

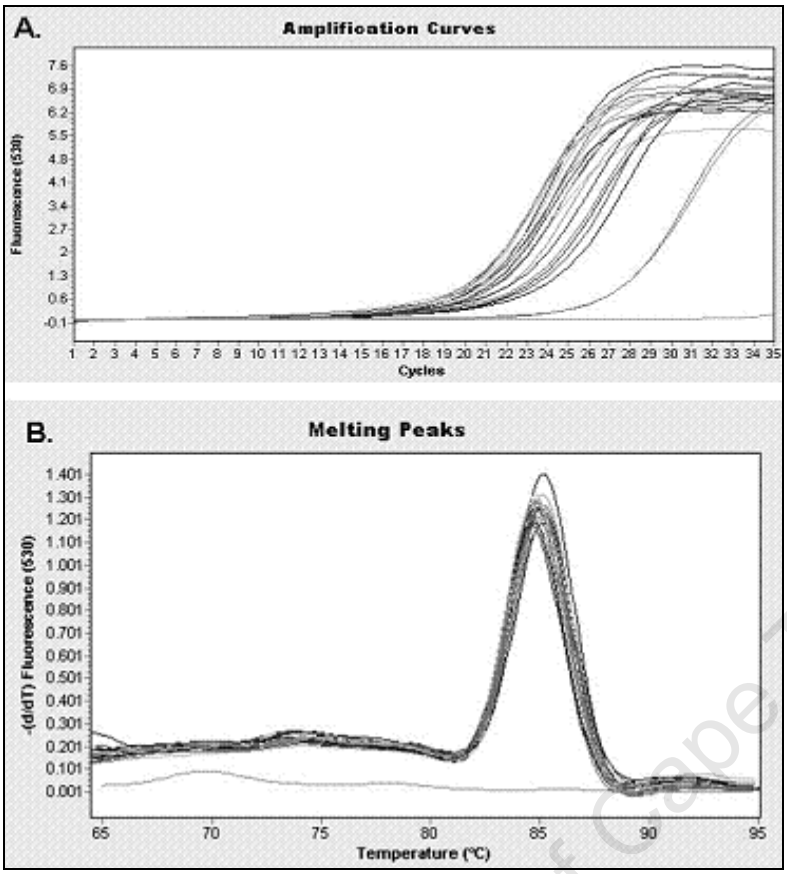

Figure 3.8: A) Amplification curves of *DAF* mRNA from the peripheral blood lymphocytes of the MG patients and normal controls. The cycle numbers are plotted on the x-axis, while the fluorescence is plotted on the y-axis. Initially, between cycles 1 and 17, there is no detectable amount of amplification product. This section is then followed by the exponential phase in which the product is detected, between cycles 18 and 26. The last phase is the plateau phase which shows that there was no significant increase in PCR product taking place (cycles 27 to 35). The experiments were performed three times and each sample was performed in duplicates. **B)** For the melting curve, temperature is plotted against the change in fluorescence with time. A single peak shows that a specific product was generated, and the absence of peaks at other temperatures shows that there were no primer dimers or other non-specific amplification products.

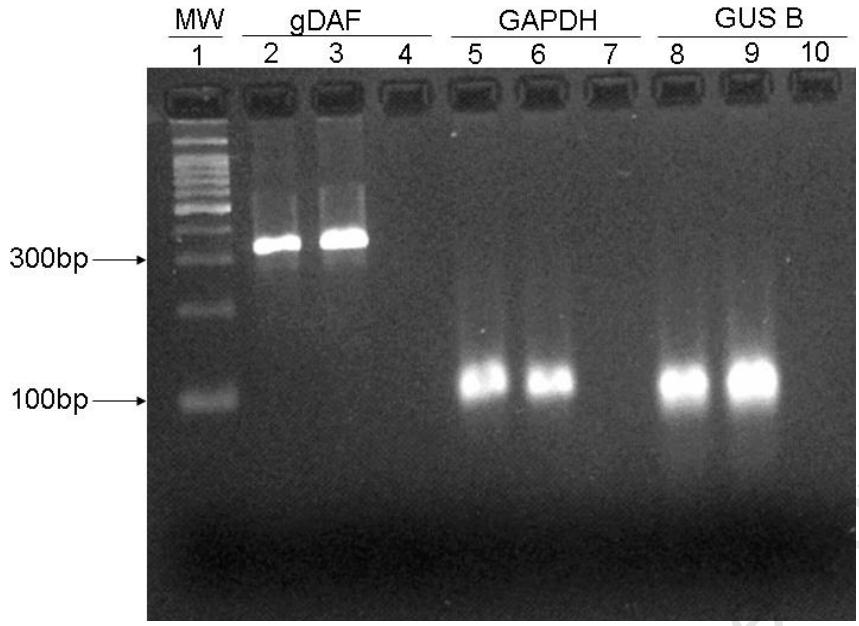

Figure 3.9: 2% agarose gel picture. 5 µl of the qRT-PCR products were run on 2% agarose gels and visualized under UV light using SYBR gold (1:2000) fluorescent dye. MW = 500 bp molecular weight marker. Lane 2 and 3 are gDAF products of approximately 322 bp. Lane 5 and 6 are GAPDH products of approximately 119 bp. Lane 8 and 9 are GUS B products of approximately 96 bp. Lane 4, 7 and 10 are water blanks for each gene amplified. Absence of a band in the water blanks shows that there was no contamination of products.

Standard curves were generated for each gene by carrying out qRT-PCR on serially diluted cDNA samples of known concentrations as mentioned in section 2.5.6. The resulting standard curves produced a linear relationship between the C_T values and the initial amount of total cDNA. Using the LightCycler machine version 4.1 software, the standard curves were constructed and the slope of the curve used to calculate the PCR efficiency. The resulting standard curves had efficiencies above 80% (gDAF 88.4%; GUS B 86.9%; and GAPDH 82.2%). The standard curve for each gene was constructed only once and used for all subsequent runs. Thus, for each consecutive qRT-PCR run one standard curve dilution sample was included in order to correct for inter-run variability. Absolute concentrations of samples in the current run could thus be read from the standard curve generated previously.

Gene expression was determined using the standard curve and the comparative 2^{-ddCT} methods (Wong and Medrano, 2005) of relative quantification. Both methods produced similar results, which were further represented in a box-and-whisker plot in **Figure 3.11**. The *DAF* mRNA expression levels in both patients and controls showed no difference in the distribution trends and no significant differences were observed (p-value > 0.05). Both sets of data were shown to follow a normal distribution by the Shapiro-Wilk test.

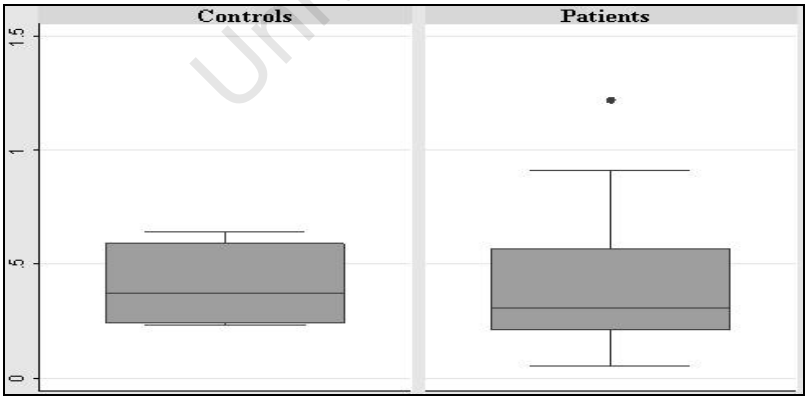

Figure 3.10: The box-and-whisker plot showing the distribution of data of the *DAF* mRNA expression in both patients (n = 11) and controls (n = 6).

3.5 The c.-198C>G increases endogenous *DAF* mRNA level in lymphoblastoid cell lines

As all MG patients were on at least one or more immunosuppressive drugs at the time of blood sampling, it was possible that variation in DAF expression between MG patients and controls was masked by the effect of the drugs on DAF. It was therefore necessary to repeat the experiment in an environment in which the effect of the drugs would be absent. This was achieved by generating lymphoblastoid cell lines using Epstein - Barr virus (EBV) transformation in an environment devoid of the MG drugs. The cell lines were transformed from the whole blood of four MG patients (**Table 3.4**), three of whom had the c-198C>G SNP and one patient who did not (WT/MG). Additionally, one further MG patient with the SNP who was not included in the previous experiment and two normal healthy controls without the SNP (WT) were also included. RNA from the cell lines was reverse transcribed into cDNA and DAF mRNA levels quantified by qRT-PCR. The results, which are representative of two independent experiments performed each time in duplicate, are shown in **Figure 3.12.** *DAF* mRNA levels were upregulated, relative to the housekeeping gene, in three MG cells lines with the c.-198C>G SNP, with only one MG4 cell line showing reduced activity. However, the MG cell line without the SNP (WT/MG) also showed increased relative DAF expression compared to the WT cell lines (**Figure 3.12**). The findings in the three MG cell lines support the luciferase promoter activity experiments performed in the COS 7, HT1080 and C2C12 cells which showed an upregulation of the promoter as a result of the c.-198C>G SNP (section 3.2). The upregulated activity in the WT/MG may be attributed to some other factor which is as yet undetermined.

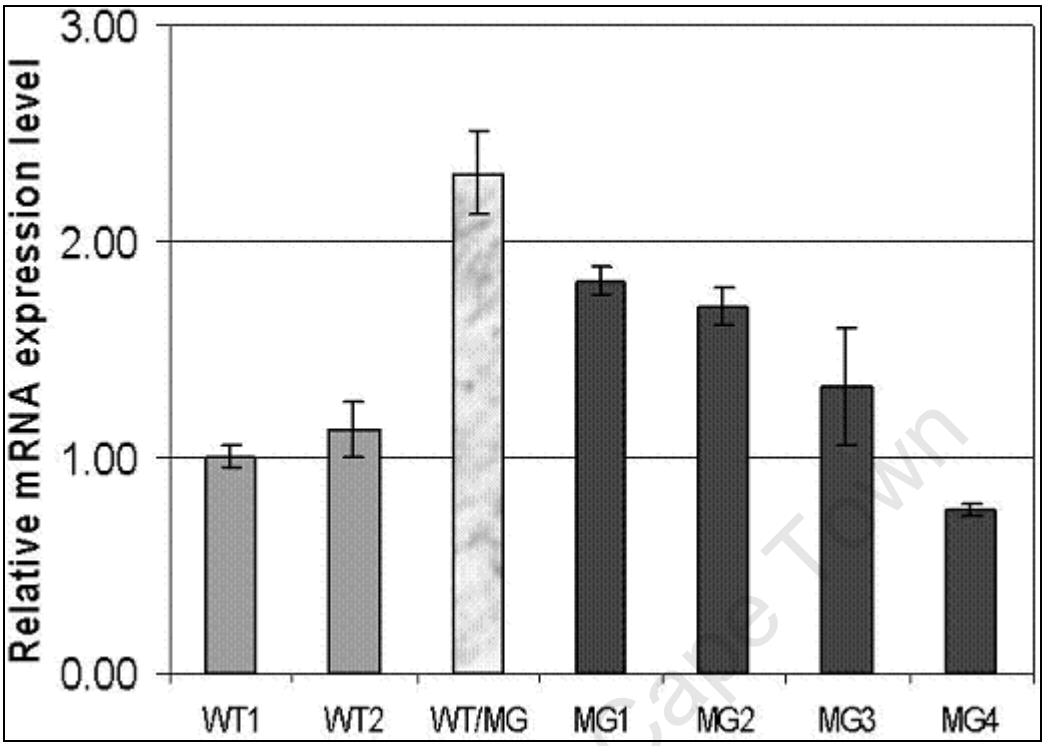

Figure 3.11: *DAF* expression in EBV transformed lymphoblastoid cell lines. Relative fold expression was normalized to the house-keeping gene GUS. The fold change was usually higher in the patient cell lines with or without the c.-198C>G (WT/MG, MG1, MG2 and MG3) than in the control cell lines (WT1 and WT2). The MG4 cell line was the odd one out with DAF mRNA expression being lower than the WT cell lines. The experiments were performed twice in duplicate.

3.6 There is a possible loss of a putative Sp1 transcription factor as a result of the c.-198C>G SNP

Once it was established that the c.-198C>G SNP generally appears to upregulate the expression and the basal promoter activity of the Mut-DAF, the next step was to predict whether the c.-198C>G change causes a loss or gain of putative transcription factor binding sites. This was achieved by searching the Consite database (http://asp.ii.uib.no:8090/cgi-bin/CONSITE/consite/) for possible transcription factor binding sites in the 5` flanking region of the DAF gene. Five Sp1 (Sp1-A to Sp1-E) binding sites were identified within 248 base pairs upstream of the ATG start codon of the WT-DAF sequence, one of which (Sp1-B) was lost when the c.-198C>G SNP was present (**Figure 3.13**). Furthermore, bioinformatic interrogations were done on the DAF promoter SNP sequence using the TRANSFAC Professional database v.11.2 (as reported in Heckmann et al. 2009) which confirmed the loss of a putative Sp1 transcription factor binding site (performed by Prof VB Bajic and Dr M Kaur from the SANBI Bioinformatics unit).

We next investigated the functional significance of losing the Sp1-B binding site by transiently co-transfecting the HT1080 cells with 150 ng of pCMV-Sp1 (a Sp1 expression plasmid) and 800 ng of WT- or Mut-DAF. Basal levels of firefly luciferase activity were measured by co-transfecting the WT- or the Mut-DAF constructs with an empty control vector (pCMV). The Sp1 expression plasmid seems to have a similar effect on both the WT- and the Mut-DAF reporters with an average of 1.5-fold increase in expression (**Figure 3.14**).

Figure 3.12: Nucleotide sequences of part of the DAF promoter region showing a total of 248 nucleotides from the initiation ATG start codon in the human *DAF* gene. The boxes show the sequences corresponding to the consensus binding site of Sp1 transcription factor. Multiple transcription start sites are shown by the arrows (Thomas and Lublin, 1993) and the main transcription start site is shown by the bent arrow (Ewulonu et al., 1991) **A)** Shows the WT-DAF promoter sequence with 5 Sp1 binding sites upstream of the ATG start codon and **B)** shows the Mut-DAF (with the c.-198C>G SNP) which has lost one Sp1 (Sp1-B) binding site at the position of the mutation (highlighted in red).

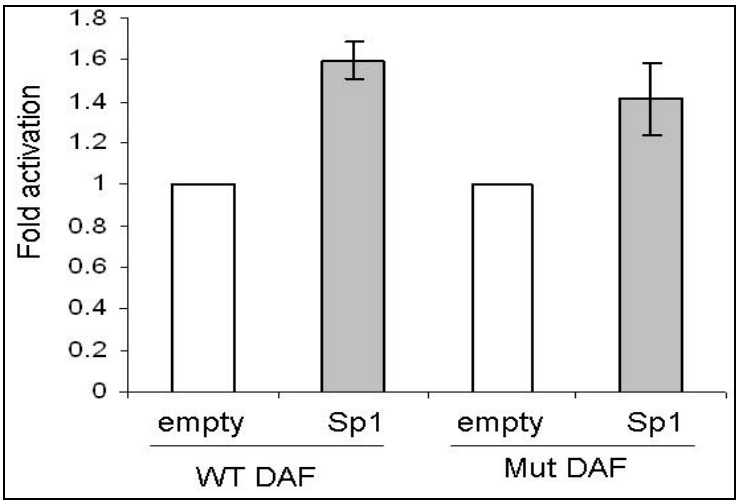

Figure 3.13: Effect of Sp1 transcription factor on the WT-DAF and the Mut-DAF. The WT- and Mut-DAF were co-transfected with the Sp1 construct or the empty (pCMV) vector into HT1080 cells. The Sp1 transcription factor had the same effect on the DAF promoter with or without the c.-198C>G SNP.

Previously, it was reported by Cauvi et al. (2006) that the two Sp1 binding sites most proximal to the transcription start site are the key Sp1 binding sites involved in the basal transcription of the mouse *Daf1* gene, whereas the third Sp1 binding site 5` of the transcription start site did not have any effect on the Daf1 promoter activity (see discussion later). In our study the lost Sp1-B binding site is the third from the transcription start site. Although we have shown that the c.-198C>G SNP does have an effect on DAF promoter activity, the results from **Figure 3.14** show that Sp1 does not appear to have a differential effect on either WT- and the Mut-DAF promoter sequences under basal conditions.

3.7 The DAF regulatory region c.-198C>G SNP influences the lipopolysaccharide (LPS-) induced DAF upregulation

Thus far we have shown that the c.-198C>G SNP is functional but we have not been able to explain the association of the observed increased basal DAF promoter activity with the loss of the putative Sp1 site. A number of studies have previously shown that LPS, which has the ability to initiate an inflammatory response, upregulates *DAF* mRNA expression levels (Iborra et al., 2003). Furthermore the LPS effect on *Daf1* gene expression was abolished by deletion of the Sp1 binding sites most proximal to the transcription start site (Cauvi et al., 2006). We next investigated the effect of LPS on *DAF* mRNA expression levels in the presence and absence of the SNP. To achieve this, the lymphoblastoid cell lines from section 3.5 were cultured with 10 µg/ml of LPS or 1x PBS (vehicle) for 6 hours and mRNA levels measured by qRT-PCR with or without LPS treatment.

In the control cell lines treated with LPS, our results showed the expected upregulation of the *DAF* mRNA expression levels. Similarly, there was increased mRNA expression in the MG patient cell line without the c.-198C>G SNP (WT/MG). However, there was a reduction in *DAF* mRNA expression levels in all the LPS treated in all the MG-SNP cell lines (**Figure 3.15 A**). These experiments were performed at least twice in duplicate.

Within a cell, an increase in transcription of a gene does not necessarily result in an increase in its protein levels. Thus, it was important to assess DAF protein levels to be sure that the reduced *DAF* mRNA transcription also results in reduced protein levels. We treated two lymphoblastoid cell lines, one WT and one MG1, with 10 µg/ml of LPS or 1x PBS for 6 hours as before. The protein was extracted under non-reducing conditions and then subjected to western blot analyses with a DAF specific antibody. All blots were re-probed with the p38 specific antibody as a loading control (**Figure 3.15B**). The results were confirmed by densitometry readings of the western blot autographs and the readings are represented in a bar graph. Quantification of the band intensities indicated a ~

2.4 fold increase and ~ 2.4 fold decrease in the protein levels of the WT and the MG1 cell lines, respectively. The WT cell line therefore showed a significant increase in protein level in response to LPS treatment whereas the protein levels were decreased in the MG cell line. These results thus supported the *DAF* mRNA expression levels observed in this study.

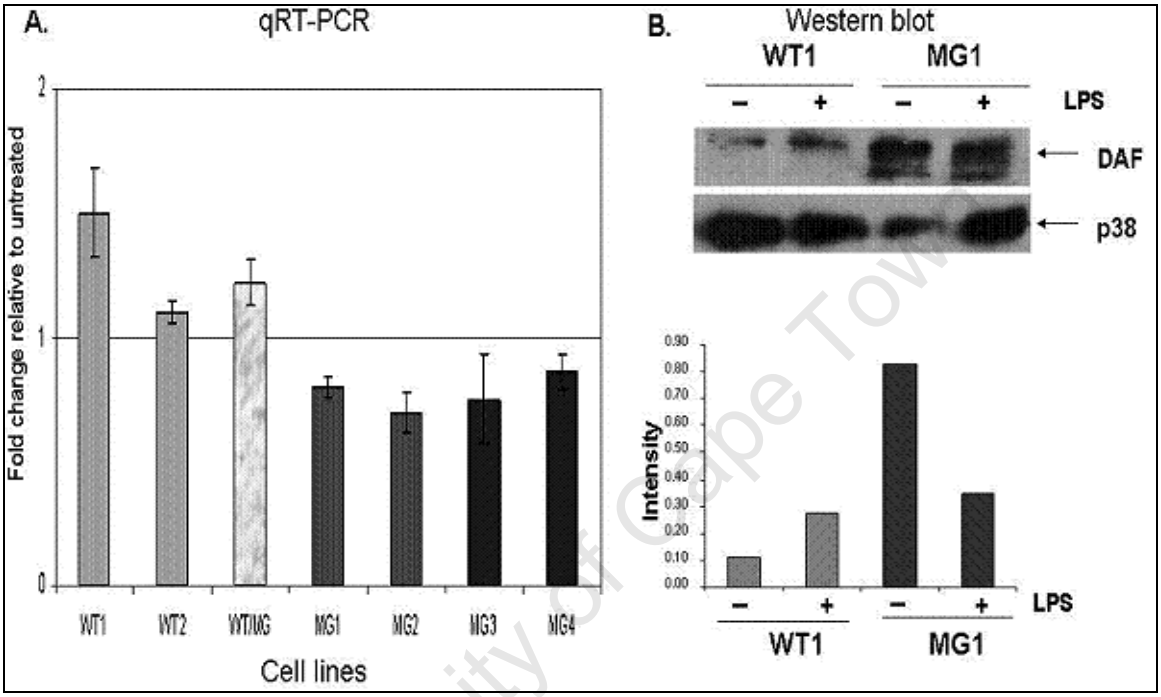

Figure 3.14: LPS treatment did not upregulate DAF expression in the SNP-lymphoblastoid cell lines. **A)** Bar graph shows the qRT-PCR results that illustrates the increased mRNA levels in the control cell lines (WT1 and WT2) and the patient cell line without the SNP (WT/MG), and the reduction in the patients with the SNP cell lines (MG1-4) in response to LPS-treatment. **B)** Western blot analysis done on the LPS-treated control and patient cell lines showed an increase in the protein levels of the LPS-treated control cell line (WT1) and a reduction in the protein levels of the SNP cell line (MG1). p38 was used as a loading control. The bar graph shows densitometry readings from the autoradiograph of DAF protein levels normalized to p38 protein levels. For the control cell line, DAF protein levels showed an increase of ~2.4 folds as a result of LPS treatment. In contrast, the MG SNP cell line showed a decrease of ~2.4 fold when treated with LPS.

3.8 Brief summary of the results

In conclusion, I have shown that the c.-198C>G SNP is associated with a severe EOM phenotype in MG patients, and that the SNP has an effect on basal expression of the *DAF* gene. I have also identified that there may be loss of a Sp1 transcription binding site in the region where the c.-198C>G SNP occurs and that this SNP led to the loss of LPS upregulation of DAF expression.

CHAPTER 4: DISCUSSION

Myasthenia gravis is an autoimmune disorder caused by abnormally activated complement producing auto-antibodies against the acetylcholine receptors (AChRs) resulting in damage at the NMJ. The classical complement pathway is controlled, in part, by regulatory proteins such as DAF which accelerate the decay of the C3 and C5 convertase complexes. Several studies in humans and mice have shown that a deficiency of DAF can result in inflammatory disorders, autoimmune disease development and susceptibility to experimental autoimmune MG (Lublin et al., 1994; Miwa and Song, 2001; Lin et al., 2004; Kaminski et al., 2006). The involvement of EOM in MG is a trademark of the condition in humans (Ubogu and Kaminski, 2001). In the EOMs of rats and mice, DAF expression is known to be generally lower than in other skeletal muscles (Porter et al., 2001) which may also be a feature of human EOM. Thus we reasoned that the MG patients developing a severe EOM phenotype may have lower background or inducible DAF expression which can lead to increased susceptibility of the EOM to complement injury. This study therefore represents the first supportive evidence for DAF's involvement in human MG pathogenesis.

A c.-198C>G SNP was detected in the 5` upstream regulatory region of the *DAF* gene and was found to be significantly associated with a severe EOM phenotype in MG individuals of African ancestry (p= 0.0003). This SNP was shown to alter the *DAF* promoter activity in three different cell lines. Transient transfections with Mut-*DAF* (having the c.-198C>G SNP) yielded approximately a 2-fold increase in the basal *DAF* promoter activity compared to WT-*DAF* in COS 7, HT 1080 and C2C12 cells. In addition, increased basal *DAF* mRNA expression was observed in three human lymphoblastoid cell lines with the SNP compared to two WT controls. The SNP was also found to alter the number of transcription factor binding sites (TFBSs) in the *DAF* 5` regulatory region. Direct matching of known TFBSs to the flanking region of the SNP showed that there is a possible loss of a putative Sp1 binding site (Heckmann et al., 2009). Co-transfection of WT- and Mut-*DAF* with Sp1 expression vectors showed that the loss of the Sp1 binding site was not critical for basal transcription of the *DAF* gene. However, the

loss of this Sp1 site was shown to down-regulate LPS-induced *DAF* mRNA expression. The findings of this study indicate that the c.-198C>G SNP influences DAF regulation, specifically the body's ability to upregulate DAF expression in response to bacterial products such as LPS, which may aggravate the progression of human myasthenic disease.

4.1 A c.-198C>G SNP associates with the severe EOM phenotype in MG

Numerous studies have shown that a single base change, also known as a SNP, in the coding region of genes may lead to a change in the amino acid sequence of the translated protein (Knight, 2003). The DAF protein CCPs 2 and 3 are important in the control of the classical complement pathway (Coyne et al., 1992) and mutations occurring in these regions disrupt the function of the CCPs in the regulation of complement activation. Deletion analysis of the STP-rich domain showed complete abolishment of DAF activity (Coyne et al., 1992) and variations in the exon encoding for the GPI-anchor attachment site may contribute towards the paroxysmal nocturnal hemoglobinuria disorder (Yazer et al., 2006). In the current study, MG patients exhibited no mutations in the exons encoding the critical domains of the *DAF* gene indicating that these protein domains are intact and probably able to perform their functions.

Promoter SNPs have been shown to influence variation in gene expression in *Drosophila* development, teleost fish populations and in human lymphoblastoid cell lines (Rifkin et al., 2003; Oleksiak et al., 2002; Cheung et al., 2003). In the past few decades these SNPs have also been implicated in susceptibility of individuals to complex diseases (Knight, 2004). We identified two SNPs in the 5`-regulatory region of the *DAF* gene, namely c.-244_-243insA and c.-198C>G. Both SNPs have previously been reported in African-American and European control populations and are designated as rs28371585 for the c.-244_-243insA (http://www.ncbi.nlm.nih.gov/projects/SNP/snp_ref.cgi?rs=28371585) and rs28371586 for the c.-198C>G SNP (http://www.ncbi.nlm.nih.gov/projects/SNP/snp_ref.cgi?rs=28371586).
Interestingly, while there is no previously reported data on South Africans, in the

present study, the Black and Mixed-Ancestry (M/A) controls independently showed similar allele frequencies for both SNPs to that found in the African American controls. Also, the South African White MG patients and controls, showed very low frequencies of the SNPs similar to the results from European control samples.

The c.-244_-243insA does not show an association with either MG or the development of ocular muscle pareses. It is therefore likely that this SNP is a common polymorphism in the 5` regulatory region of the *DAF* gene and may be nonpathogenic.

Overall, the c.-198C>G SNP showed no significant association with MG compared with controls. However, when the patients were categorised on the basis of severity of the EOM, a significant association was seen between the c.-198C>G SNP and patients developing the treatment-resistant EOM phenotype. It appears that the Black (OR = 12.9, p = 0.006) and M/A (OR = 6.2, p = 0.022) subjects with the SNP are more susceptible to developing MG with at least one or more EOM dysfunction compared to the racially matched controls. An even stronger association is observed between the c.-198C>G SNP and this clinical phenotype when the Black and M/A patient categories are combined in an African ancestry group (OR of 8.6 (p = 0.0003)). These findings suggest that the c.-198C>G SNP may be a susceptibility allele for the development of the severe EOM phenotype associated with MG. Alternatively, the SNP may not be the susceptibility allele but its association with this MG phenotype may imply that it is in linkage disequilibrium with an, as yet, unknown disease-causing allele on the same chromosome.

4.2 Regulatory effect of the *DAF* c.-198C>G SNP

The initial hypothesis of this study was that DAF expression may be lower than normal in the MG patients with severe EOM phenotype rendering their eye

muscles vulnerable to complement damage. The activation of the basal *DAF* promoter activity was therefore unexpected. One possible explanation for this upregulation may be that during the design of the reporter gene construct other unexpected variations in the sequence may have been introduced. However, the sequences were verified after site-directed mutagenesis, thus excluding this possibility. Another possible explanation is that the reporter gene assays are highly dependent on biological systems in which the experiments are performed (Knight, 2004). In this study the promoter reporter assays were performed in COS-7 monkey epithelial cells, HT1080 human fibrosarcoma cells, and C2C12 mouse myoblast cells, all of which may not be representative of the EOM system. In the absence of a better representative of the in vivo EOM tissue, basal *DAF* mRNA expression was analysed in three lymphoblastoid cell lines derived from MG patients with the c.-198C>G SNP. These results showed that DAF was upregulated in the SNP cell lines compared to the controls. It is known that constitutive DAF expression is tissue- and cell-type specific (Lin et al., 2001; Thomas and Lublin, 1993) and that it is regulated by various cytokines, prostaglandins and tissue-specific factors (reviewed in Cauvi et al., 2006). Therefore, basal transcription in the MG individuals with the SNP may theoretically be influenced by certain circumstances that may differ from an in vitro situation.

The lack of variation in *DAF* mRNA expression in peripheral blood from patients and controls was thought to be the effect of the immunosuppressive drugs. It was reasoned that lymphoblastoid cell lines (LCLs) would be a more appropriate drug-free system for studying endogenous DAF expression. LCLs, which express endogenous DAF (Tate et al., 1989), were established from B lymphocytes of individuals with and without the c.-198C>G SNP, using EBV-transformation. The EBV infects the B lymphocytes and transforms them by changing cellular gene expression through incorporation and expression of several viral proteins capable of causing continuous B-cell proliferation (Rickinson and Kieff, 2001). Surprisingly, when comparing the c.-198C>G SNP to WT cell lines, the relative *DAF* mRNA levels under basal conditions also showed

increased level of expression in three lymphoblastoid cell lines, with an exception of one cell line (MG4) (**Figure 3.12**). These results were similar to the luciferase reporter assays which showed upregulation of basal transcription of the *DAF* reporter vector in the presence of the c.-198C>G SNP. Unexpectedly, *DAF* mRNA levels were also upregulated in the WT/MG lymphoblasts (without the SNP), which may implicate some other, as yet, unknown factor.

Studies have shown that SNPs in the 5` regulatory region of a gene can be either cis-acting or trans-acting (Tegeder et al., 2006). The cis-acting SNPs influence the gene expression of that specific gene whereas trans-acting SNPs may affect the expression of another gene (Knight, 2004). The c.-198C>G SNP may be a cis-acting regulatory SNP as it affects the transcriptional regulation of the *DAF* gene. Interestingly, the SNP also appears to be in a region that has been shown to harbour several transcriptional control elements in both humans and mice. Ewulonu et al. (1991) demonstrated that there are inhibitory regulatory sequences in the *DAF* promoter and showed that *DAF* activity can be reduced to 11% or less in COS cells if the sequence between -159 and -242 from the start codon is deleted. In addition, deletion of the region between -207 and -77 in the human *DAF* gene resulted in approximately 75% loss of transcriptional activity (Thomas and Lublin, 1993). In the mouse *daf1* gene, this region was also shown to contain enhancer elements similar to those in the human *DAF* (Cauvi et al., 2006). Therefore, a change in one base in the regulatory region, such as the c.-198C>G SNP, may lead to a gain of an enhancer or loss of an inhibitory element, possibly resulting in the activation in *DAF* promoter activity.

In this study, computational methods predicted the loss of a Sp1 binding site in the region of the c.-198C>G SNP. The Sp1 transcription factor is a member of the four small proteins Sp-family of transcription factors consisting of Sp1, Sp2, Sp3 and Sp4 that contain three zinc fingers near the C-terminus and is ubiquitously expressed (Suske, 1999). The Sp1 transcription factor has been shown to activate gene promoters through the GC-boxes (Pascal and Tjian, 1991) and therefore is important in the basal transcription of GC-rich, TATA-less

genes such as mouse *Daf*1 gene, house-keeping genes, tissue-specific genes and genes involved in growth regulation (Suske, 1999; Philipsen and Suske, 1999; Cook et al., 1998). There is evidence that clusters of Sp1 binding sites are required for efficient transcription of the TATA-less promoter for insulin-like growth-factor binding-2 protein in rats (Boisclair et al., 1993).

4.3 Loss of the Sp1 site affects LPS-induced DAF upregulation in humans

In mouse studies, Cauvi et al. (2006) identified three Sp1 binding sites in the *DAF*1 promoter (+1 to -619) and deletion of the most distal Sp1 site (equivalent to that lost in this study) did not have a significant effect on the basal transcription of the *daf1* gene. Interestingly, in the same study however, deletion of the Sp1 site which is equivalent to the putative Sp1 site at c.-198C>G SNP showed upregulation of luciferase reporter activity compared to the wild type in a murine B-cell line (M12.4). In the present study, transient co-transfections with a Sp1 expression vector showed a similar effect on both the WT- and Mut-*DAF* promoter constructs, suggesting that the Sp1 site at -198 position may not be important for basal transcription. It is also possible that endogenous Sp1 is present in great abundance and therefore masks the effect of transfected Sp1 protein.

Various complement regulatory proteins, such as DAF, are reportedly upregulated in response to LPS in endometrial cells (Iborra et al., 2003) and rat smooth muscle cells (Li et al., 1999). Cauvi et al. (2006) showed that this LPS upregulation is mediated through Sp1 binding sites in B-cells and macrophages, but not fibroblasts, suggesting tissue specificity of LPS-induced DAF upregulation. Sequential deletion of Sp1 sites, particularly those close to the transcription start site showed loss of upregulation in response to LPS (Cauvi et al., 2006). Similarly, the results of this study show that lymphoblasts of individuals with WT-DAF showed upregulation of *DAF* mRNA expression (**Figure**

3.15A). However, *DAF* mRNA and protein levels were not responsive to LPS in the lymphoblastoid cells of the MG patients with the c.-198C>G SNP (**Figure 3.15**). These results suggest that the loss of the putative Sp1 binding site at c.-198C>G may affect the upregulation of DAF in response to LPS providing further supportive evidence that the c.-198C>G SNP has functional significance.

LPS is a component of the cell wall of gram-negative bacteria that has the ability to initiate inflammatory responses (Antonicelli et al., 2004). Activation of the early proteins of the classical and alternative pathways of complement has been shown to produce proteolytic peptides with inflammatory activities (Frank, 1995), and activation of the late complement proteins leads to the formation of terminal complement complexes which associate with inflammatory cells and can be damaging to the host tissues (reviewed in Lang et al., 1997). These terminal complement complexes together with C3 fragments have been observed at NMJs in affected muscles of MG (Sahashi et al., 1980). As a potent inhibitor of C3 and C5 convertases, the inability of DAF to upregulate under inflammatory conditions, such as mimicked by LPS, may indicate that the MG patients with the c.-198C>G SNP are unable to express adequate membrane-bound DAF resulting in severe complement mediated injury at the EOM in such circumstances. Indeed, in the DAF knock-out mouse model, *daf1*-deficient mice were more susceptible to EAMG induction and suffered more severe complement mediated muscle damage compared to wild-type mice (Lin et al., 2002).

There is evidence to show that DAF has another function apart from complement. Liu et al. (2005) showed that *daf1* deficiency in mice led to the development of enhanced T-cell immune responses and Heeger et al. (2005) also showed that the absence of Daf resulted in loss of normal T-cell regulation which in turn caused local inflammation. In addition, T-cell immunity has also been shown to be involved in the pathogenicity of MG, as mice that lacked CD4+ T-cell receptors did not develop EAMG (Kaul et al., 1994). We therefore speculated that reduced DAF, caused by the c.-198C>G SNP, may aggravate

immune-mediated damage to EOM in MG independent from its effect on complement.

4.4 Limitations to the study

The tissue specificity of DAF regulation in the EOMs could not be demonstrated as it is impossible to obtain EOMs from the MG patients specifically at an active stage of the disease. The COS-7, HT1080, C2C12 and human lymphoblastoid cell lines may not be ideal for illustrating the effect of the *DAF* c.-198C>G SNP in the human EOM environment in vivo.

In this study the loss of the Sp1 transcription factor binding site due to the c.-198C>G SNP was investigated. This polymorphism however also resulted in a gain of a putative NF-$_K$B transcription factor binding site which has been implicated in inflammatory conditions. However, due to time constraints the gain of the NF-$_k$B binding site could not be investigated.

Ideally the effect of the SNP on DAF expression should be examined in MG patients before exposure to therapeutic drugs which probably influences gene expression. Unfortunately the project was initiated during the course of treatment and thus this was not possible.

4.5 Conclusion

This project focused on investigating a "complement hypothesis" in which reduced DAF expression results in a treatment-resistant EOM phenotype in a subgroup of MG patients. The experimental findings reported in this thesis contribute considerably to the existing knowledge of MG pathogenecity. For the first time, it is shown that a SNP in the regulatory region of the human DAF gene influences DAF expression. The observed upregulation of the gene expression contradicted the initial hypothesis, probably because the experimental conditions were not representative of the in vivo EOM tissue. However, in conditions mimicking the inflammatory environment of an autoimmune disorder DAF expression was down-regulated as hypothesised. Thus it can be deduced that the SNP may indeed reduce DAF expression and consequently reduce the

protection of tissues against complement-mediated damage. Current treatments are aimed at reducing the production of auto-antibodies but this is not specifically targeting the prevention of complement mediated damage. It therefore seems prudent to suggest that in MG patients who develop a treatment-resistant EOM phenotype and who are found to have the c.-198C>G SNP, additional anti-complement therapy should be considered.

REFERENCES

- Abbott RJM, Spendlove I, Roversi P, Fitzgibbon H, Knott V, Teriete P, McDonnell JM, Handford PA, Lea SM. Structural and functional characterization of a novel T cell receptor co-regulatory protein complex, CD97-CD55. J. Biol. Chem. 282:22023-22032, 2007.
- Ahearn JM, Fearon DT. Structure and function of the complement receptors, CR-1 (CD35) and CR-2 (CD21). Adv. Immunol. 6:183-219, 1989.
- Antonicelli F, Brown D, Parmentier M, Drost EM, Hirani N, Rahman I, Donaldson K, MacNee W. Regulation of LPS-mediated inflammation in vivo and in vitro by the thiol antioxidant Nacystelyn. Am. J. Physiol. Lung. Cell. Mol. Physiol. 286: L1319-L1327, 2004.
- Asch AS, Kinoshita T, Jaffe EA, Nussenzweig V. Decay-accelerating factor is present on cultured human umbilical vein endothelial cells. J. Exp. Med. 163:221-226, 1986.
- Barilla-LaBerea ML, Liszewski MK, Lambris JD, Hourcade D, Atkinson JP. Role of membrane cofactor protein (CD46) in regulation of C4b and C3b deposited on cells. J. Immunol. 68(12):6298-6304, 2002.
- Bateman KJ, Schinkel M, Little F, Liebenberg L, Vincent A, Heckmann JM. Incidence of seropositive myasthenia gravis in Cape Town and South Africa. S. Afr. Med. 97:630-634, 2005.
- Boisclair YR, Brown AL, Casola S, Rechler MM. Three clustered Sp1 sites are required for efficient transcription of the TATA-less promoter of the gene for insulin-like growth factor-binding protein-2 from the rat. J. Biol. Chem. 268:24892-24901, 1993.
- Brodbeck WG, Kuttner-Kondo L, Mold C, Medof ME. Structure/Function studies of human decay-accelerating factor. Immunology 101:104-111, 2000.
- Brodbeck WG, Liu D, Sperry J, Mold C, Medof ME. Localization of classical and alternative pathway regulatory activity within the decay-accelerating factor. J. Immunol. 156: 2528–33, 1996.

- Campbell H, Rudan I. Interpretation of genetic association studies in complex disease. Pharmacogenomics J. 2:349-360, 2002.
- Cardon LR, Bell JI. Association study designs for complex diseases. Nat. Rev. Gen. 2: 91-99, 2001.
- Caras IW, Gregory N, Weddel GN. Signal peptide for protein secretion directing glycophospholipid membrane anchor attachment. Science 243:1196-1198, 1989.
- Cauvi DM, Cauvi G, Pollard KM. Constitutive expression of murine decay-accelerating factor 1 is controlled by the transcription factor Sp1. J. Immunol. 177:3837-3847, 2006.
- Cheung VG, Conlin LK, Weber TM, Arcaro M, Jen KY, Morley M, Spielman RS. Natural variation in human gene expression assessed in lymphoblastoid cells. Nat. Genet. 33: 422-425, 2003.
- Conti-Fine BM, Milani M, Kaminski HJ. Myasthenia gravis: past, present, and future. J. Clin. Invest. 116:2843-2854, 2006.
- Coyne KE, Hall SE, Thompson S, Arce MA, Kinoshita T, Fujita T, Anstee DJ, Rosse W, Lublin DM. Mapping of epitopes, glycosylation sites, and complement regulatory domains in human decay-accelerating factor. J. Immunol. 149:2906-2913, 1992.
- Cook T, Gebelein B, Mesa K, Mladek A, Urrutia R. Molecular cloning and characterization of TIEG2 reveals a new subfamily of transforming growth factor-ß-inducible Sp1-like zinc finger-encoding genes involved in the regulation of cell growth. J. Biol. Chem. 273:25929-25936, 1998.
- Daniels GL, Green CA, Mallinson G, Okubo Y, Hori Y, Kataoka A, Kaihara M. Decay-accelerating factor (CD55) deficiency phenotypes in Japanese. Transfus. Med. 8(2):141-147, 1998.
- Eisenberg E, Levanon EY. Human housekeeping genes are compact. Trend in Genetics. Volume 19 No 7, 2003.
- Engel AG, Sahashi K, Lambert EH, Howard FH. Ultrastructural localization of the acetylcholine receptor, immunoglobulin G and the third and ninth

complement components at the motor endplate and their implications for the pathogenesis of myasthenia gravis. In: A.J. Aguyo and G. Karpati (Eds.) Current topics in nerve and muscle research. Excerpta Medica, Amsterdam, 111-122, 1979.

- Ewulonu UK, Ravi L, Medof ME. Characterization of the decay-accelerating factor gene promoter region. Proc. Natl. Acad. Sci. 88:4675-4679, 1991.
- Fazekas A, Komoly S, Boszik B, Szobor A. Myasthenia gravis: Demonstration of membrane attack complex in muscle endplates. Clin. Neuropathol. 5:78-83, 1986.
- Frank M. Complement system, in Samter's immunologic diseases. Little and Brown, Boston, 331-352, 1995.
- Giulietti A, Overberg L, Valckx D, Decallonne B, Bouillon R, Mathieu C. An overview of real-time quantitative PCR: applications to quantify cytokine gene expression. Methods 25:386-401, 2001.
- Halstensen, T. S., T. E. Mollnes, P. Garred, O. Fausa, and P. Brandtzaeg. Surface epithelium related activation of complement differs in Crohn's disease and ulcerative colitis. Gut 33:902-908, 1992.
- Hamann J, Vogel B, van Schijndel GM, van Lier RA. The seven-span transmembrane receptor CD97 has a cellular ligand (CD55, DAF). J. Exp. Med. 184:1185-1189, 1996.
- Harris CL, Hanna SM, Mizuno M, Holt DS, Marchbank KJ, Morgan BP. Characterization of the mouse analogues of CD59 using novel monoclonal antibodies: tissue distribution and functional comparison. Immunology 109:117-126, 2003.
- Heckmann JM, Bryer A, Greenberg LJ. When is it not Huntington's disease? S. Afr. Med. J. 91:132-133, 2001.
- Heckmann JM, Owen EP, Little F. Myasthenia gravis in South Africans: Racial differences in clinical manifestations. Neuromusc. Dis. 17:929-934, 2007.
- Heckmann JM, Uwimpuhwe H, Ballo R, Kaur M, Bajic VB, Prince S. A functional SNP in the regulatory region of the decay accelerating factor gene

- Heeger PS, Lalli PN, Lin F, Valujskikh A, Liu J, Muqim N, Xu Y, Medof ME. Decay accelerating factor modulates induction of T cell immunity. J. Exp. Med. 201:1523-1530, 2005.
- Higuchi R, Dollinger G, Walsh PS, Grifith R. Simultaneous amplification and detection of specific DNA sequences. Biotechnology 10: 413-417, 1992.
- Hoffmann EM. Inhibition of complement by a substance isolated from human erythrocytes. I. Extraction from human erythrocyte stromata. Immunochemistry 6:391-403, 1969.
- Holla VR, Wang D, Brown JR, Mann JR, Katkuri S, DuBois RN. Prostagladin E_2 regulates the complement inhibitor CD55/decay-accelerating factor in colorectal cancer. J. Biol. Chem 280:476-483, 2005.
- Hughes BW, Kusner LL, Kaminski HJ. Molecular architecture of the neuromuscular junction. Muscle nerve 33: 445-461, 2006.
- Iborra A, Mayorga M, Llobet N, Martinez P. Expression of complement regulatory proteins [membrane cofactor protein (CD46), decay accelerating factor (CD55), and protectin (CD59)] in endometrial stressed cells Cell Immunol. 223:46-51, 2003.
- Kaminski HJ. Myasthenia gravis and related disorders. Humana Press, Inc., Totowa, 1-396, 2003.
- Kaminski JH, Li Z, Richmonds C, Lin F, Medof ME. Complement regulators in extraocular muscle and experimental autoimmune myasthenia gravis. Exp. Neurol. 189:333-342, 2004.
- Kaminski JH, Kusner LL, Richmonds C, Medof ME, Lin F. Deficiency of decay accelerating factor and CD59 leads to crisis in experimental myasthenia. Exp. Neurol. 202:287-293, 2006.
- Kaul R, Shenoy M, Goluszko E, Christadoss P. Major histocompatibility complex II gene disruption prevents experimental autoimmune myasthenia gravis. J. Immunol. 152:3152-3157, 1994.

- Keesey JC. “Crisis” in myasthenia gravis: an historical perspective. Muscle nerve 26:1-3, 2002.
- Kendall G, Crankson H, Ensor E, Lublin DM, Latchman DS. Activation of the gene encoding decay accelelrating factor following nerve growth factor treatment of sensory neurons is mediated by promoter sequences within 206 bases of the transcriptional start site. J. Neurosci Res 45:96-103, 1996.
- Khanna S, Porter JD. Conservation of synapse-signaling pathways at the extraocular muscle neuromuscular junction. Ann. N.Y. Acad. Sci. 956:394-396, 2002.
- Khanna S, Richmonds CR, Kaminski HJ, Porter JD. Molecular organization of the extraocular muscle neuromuscular junction: Partial conservation of and divergence from the skeletal muscle prototype. Invest. Ophthalmol. Vis. Sci. 44:1918-1926, 2003.
- Kim DD, Song WC. Membrane complement regulatory proteins. Clin. Immunol. 118:127-136, 2006.
- Kinoshita T, Medof ME, Silber R, Nussenzweig V. Distribution of decay-accelerating factor in the peripheral blood of normal individuals and patients with paroxysmal nocturnal hemoglobinuria. J. exp. Med. 162:75, 1985.
- Knight JC. Functional implications of genetic variation in non-coding DNA for disease susceptibility and gene regulation. Clin. Sci. 104:493-501, 2003.
- Knight JC. Regulatory polymorphisms underlying complex disease traits. J. Mol. Med. 83:97-109, 2004.
- Kohl J. Self, non-self, and danger: a complementary view. Adv. Exp. Med. Biol. 586:71-94, 2006.
- Kubo Y. Comparison of initial staged of muscle differentiation in rat and mouse myoblastic and mouse mesodermal stem cell lines. J. Physiol. 442:743-759, 1991.
- Kuttner-Kondo LA, Mitchell L, Hourcade DE, Medof ME. Characterization of the active sites in decay-accelerating factor. J. Immunol. 167:2164-2171, 2001.

- Lang TJ, Badea TC, Wade R, Shin ML. Sublytic terminal complement attack on myotubes decreases the expression of mRNAs encoding muscle-specific proteins. J. Neurochem. 68:1581-1589, 1997.
- Lass JH, Walter EI, Burris TE, Grossniklous HE, Roat MI, Skelnik DL, Needham L, Singer M, Medof ME. Expression of two molecular forms of the complement decay-accelerating factor in the eye and lacrimal gland. Invest. Ophthalmol. Vis. Sci. 31:1136-1148, 1990.
- Lennon VA, Seybold ME, Lindstrom JM, Cochrane C, Ulevitch R. Role of complement in the pathogenesis of experimental autoimmune myasthenia gravis. J. Exp. Med. 147:973-983, 1978.
- Li W, Tada T, Miwa T, Okada N, Ito J, Okada H, Tateyama H, Eimoto T. mRNA expression of complement components and regulators in rat arterial smooth muscle cells. Microbiol. Immunol. 43:585-593, 1999.
- Lin F, Fukuoka Y, Spicer A, Ohta R, Okada N, Harris CL, Emancipator SN, Medof ME. Tissue distribution of products of the mouse decay accelerating factor (DAF) genes: exploitation of a Daf1 knock-out mouse and site-specific monoclonal antibodies. Immunology 108:215-225, 2001.
- Lin F, Kaminski HJ, Conti-Fine BM, Wang W, Richmonds C, Medof ME. Markedly enhanced susceptibility to experimental autoimmune myasthenia gravis in the absence of decay-accelerating factor protection. J. Clin. Inves. 110:1269-1274, 2002.
- Lin F, Spenser D, Hatala DA, Levine AD, Medof ME. Decay-accelerating factor deficiency increases susceptibility to dextran sulfate sodium-induced colitis: Role for complement in inflammatory bowel disease. J. Immunol. 172:3836-3841, 2004.
- Liszewski MK, Post TW, Atkinson JP. Membrane cofactor protein (MCP or CD46): newest member of the regulators of the complement activation gene cluster. Annu. Rev. Immunol. 9:431-455, 1991.
- Liu J, Miwa T, Hilliard B, Chen Y, Lambris JD, Wells AD, Song WC. The complement inhibitory protein DAF (CD55) suppresses T cell immunity in vivo. J. Exp. Med. 201:567-577, 2005.

- Lublin DM, Atkinson JP. Decay-accelerating factor: biochemistry, molecular biology, and function. Annu. Rev. Immunol. 7:35, 1989.
- Lublin DM, Lemons RS, Le Beau MM, Holers VM, Tykocinski ML, Medof ME, Atkinson JP. The gene encoding decay-accelerating factor (DAF) is located in the complement-regulatory locus on the long arm of chromosome 1. J. exp. Med. 165:1731-36, 1987.
- Lublin DM, Mallinson G, Poole J, Reid ME, Thompson ES, Ferdman BR, Telen MJ, Anstee DJ, Tanner MJA. Molecular basis of reduced or absent expression of decay-accelerating factor in Cromer blood group phenotypes. Blood 84:1276-1282, 1994.
- Luretta KL. Statistical primer for cardiovascular research: Genetic association studies. Circulation 118:96-101, 2008.
- Matys V, Kel-Margoulis OV, Fricke E, Liebich I, Land S, Barre-Dirrie A, Reuter I, Chekmenev D, Krull M, Hornischer K, Voss N, Stegmaier P, Lewicki-Potapov B, Saxel H, Kel AE, Wingender E. TRANSFAC and its module TRANSCompel: transcriptional gene regulation in eukaryotes. Nucl. Acids Res. 34 (Database issue):D108-110, 2006.
- Medof ME, Walter EI, Rutgers JL, Knowles DM, Nussenzweig V. Identification of decay-accelerating factor (DAF) on epithelium and glandular cells and in body fluids. J. exp. Med. 165:848-864, 1987.
- Miwa T, Maldonado MA, Zhou L, Yamada K, Gilkeson GS, Eisenberg RA, Song WC. Decay-accelerating factor ameliorates systemic autoimmune disease in MRL/lpr mice via both complement-dependent and –independent mechanisms. Am. J. Pathol. 170(4):1258-1266, 2007.
- Miwa T, Song WC. Membrane complement regulatory proteins: insight from animal studies and relevance to human diseases. Int. J. Immunopharmacol. 1:445-459, 2001.
- Murray KP, Mathure S, Kaul R, Khan S, Carson LF, Twiggs LB, Martens MG, Kaul A. Expression of complement regulatory proteins-CD35, CD46, CD55, and CD59-in benign and malignant endometrial tissue. Gynecol. Oncol. 76:176-182, 2000.

- Nakano S, Engel AG. Quantitative immunocytochemical analysis of inflammatory cells and detection of complement membrane attack complex at the end-plate of 30 patients. Neurology 43:1167-1172, 1993.
- Nicholson-Weller A, Burge J, Fearon DT, Weller PF, Austen KF. Isolation of a human erythrocyte membrane glycoprotein with Decay accelerating activity for C3 convertases of the complement system. J. Immunol. 129:184, 1982.
- Nicholson-Weller A, March JP, Rosen CE, Spicer DB, Austen KF. Surface membrane expression by human blood leukocytes and platelets of decay-accelerating factor, a regulatory protein of the complement system. Blood 65:1237-1244, 1985.
- Nussenweig V. Inhibition of complement activation on the surface of cells after incorporation of decay-accelerating factor (DAF) into their membranes. J. exp. Med. 160:1558-78, 1984.
- Okada N, Harada R, Fujita T, Okada H. A novel membrane glycoprotein capable of inhibiting membrane attack by homologous complement. Int. Immunol. 1:205-208, 1989.
- Oleksiak MF, Churchill GA, Crawford DL. Variation in gene expression within and among natural populations. Nat. Genet. 32:261-266, 2002.
- Osuka F, Endo Y, Higuchi M, Suzuki H, Shio Y, Fujiu K, Kanno R, Oishi A, Terashima M, Fujita T, Gotoh M. Molecular cloning and characterization of novel splicing variants of human decay-accelerating factor. Genomics 88:316-322, 2006.
- Pascal E, Tjian R. Different activation domains of Sp1 govern formation of multimers and mediate transcriptional synergism. Genes Dev. 5:1646-1656, 1991.
- Philipsen S, Suske G. A tale of three fingers: the family of mammalian Sp/XKLF transcription factors. Nucleic Acids Res. 27:2991-3000, 1999.
- Piddlesden SJ, Jiang S, Levin JL, Vincent A, Morgan BP. Soluble complement receptor 1 (sCR1) protects against experimental autoimmune myasthenia gravis. J. Neuroimmunol. 71, pp 173-177, 1996.

- Porter JD, Khanna S, Kaminski HJ, Merriam AP, Richmonds CR, Leahy P, Andrade FH. Extraocular muscle is defined by a fundamentally distinct gene expression profile. Proc. Natl. Accad. Sci. U.S.A. 98:12062-12067, 2001.
- Post TW, Arce MA, Liszewski MK, Thompson ES, Atkinson JP, Lublin DM. Structure of the gene for human complement protein decay-accelerating factor. J. Immunol. 144:740-744, 1989.
- Qian YM, Qin X, Miwa T, Sun X, Halperin JA, Song WC. Identification and characterization of a new gene encoding the mouse terminal complement inhibitor CD59. J. Immunol. 165:2528-2534, 2000.
- Qin X, Miwa T, Aktas H, Gao M, Lee C, Qian YM, Morton CC, Shahsafaei A, Song WC, Halperin JA. Genomic structure, functional comparison, and tissue distribution of mouse Cd59a and Cd59b. Mamm. Genome 12:582-589, 2001.
- Rainen L, Oelmueller U, Jurgensen S, Wyrich R, Ballas C, Schram J, Herdman C, Bankaitis-Davis D, Nicholls N, Trollinger D, Tryon V. Stabilization of mRNA expression in whole blood samples. Clin. Chem. 48: 1883-1890, 2002.
- Rickinson, A., and Kieff E**.** Epstein-Barr virus. *In* D. Knipe, P. Howley, D. Griffin, M. Martin, R. Lamb, B. Roizman, and S. Straus (ed.), Fields virology, 4th ed., vol. 2. Lippincott Williams and Wilkins, Philadelphia, Pa, 2575-2628, 2001.
- Rifkin SA, Kim J, White KP. Evolution of gene expression in the Drosophila melanogaster subgroup. Nat. Genet. 33:138-144, 2003.
- Rodriguez-Murillo L, Greenberg DA. Genetic association analysis: a primer on how it works, its strengths and its weaknesses. Int. J. Androl. 31:546-556, 2008.
- Rollins SA, Sims PJ. The complement-inhibitory activity of CD59 resides in its capacity to block incorporation of C9 into membrane C5b-9. J. Immunol. 144:3478-3483, 1990.
- Rosse WF, Nishimura J. Clinical manifestations of paroxysmal nocturnal hemoglobinuria: present state and future problems. Int. J. Hematol. 77:113-120, 2003.

- Sahashi K, Engel AG, Linstrom JM, Lambert EH, Lennon VA. Ultrastructural localization of immune complexes (IgG and C3) at the end-plate in experimental autoimmune myasthenia gravis. J. Neuropathol. Exp. Neurol. 37:212-213, 1978.
- Sahashi K, Engel AG, Lambert EH, Howard Jr FM. Ultrastructural localization of the terminal and lytic ninth complement component (C9) at the motor end-plate in myasthenia gravis. J. Neuropathol. Exp. Neurol. 39:160-172, 1980.
- Soltys J, Gong B, Kaminski JH, Zhou Y, Kusner LL. Extraocular muscle susceptibility to Myasthenia gravis. Unique immunological Environment? Ann. N.Y. Acad. Sci. 1132:220-224, 2008.
- Spicer AP, Seldin MF, Gendler SJ. Molecular cloning and chromosomal localisation of the mouse decay-accelerating factor genes. Duplicated genes encode glycosylphosphatidylinositol-anchored and transmembrane forms. J. Immunol. 1355:3079-3091, 1995.
- Suske G. The Sp1-family of transcription factors. Gene 238:291-300, 1999.
- Tate CG, Uchikawa M, Tanner MJA, Judson PA, Parsons SF, Mallinson G, Anstee DJ. Studies on the defect which causes absence of decay accelerating factor (DAF) from the peripheral blood cells of an individual with the Inab phenotype. Biochem. J. 261:489, 1989.
- Tegeder I, Costigan M, Griffin RS, Abele A, Belfer I, Schmidt H, Ehnert C, Nejim J, Marian C, Scholz J, Wu T, Allchome A, Diatchenko L, Binshtok AM, Goldman D, Adolph J, Sama S, Atlas SJ, Carlezon WA, Parsegian A, Lotsch J, Fillingim RB, Maixner W, Giesslinger G, Max MB, Woolf CJ. GTP cyclohydrolase and tetrahydrobiopterin regulate pain sensitivity and persistence. Nat. Med. 12:1269-1277, 2006.
- Thomas DJ and Lublin DM. Identification of the 5'-flanking regions affecting the expression of the human decay accelerating factor gene and their role in tissue-specific expression. J. Immunol. 150:151-160, 1993.
- Ubogu U, Kaminski JH. Preferential involvement of extraocular muscle by myasthenia gravis. Neuroophthalmology 25:219-228, 2001.

- Ueki T, Mizuno M, Uesu T, Kiso T, Nasu J, Inaba T, Kihara Y, Mastuoka Y, Okada H, Fujita T, Tsuji T. Distribution of activated complement, C3b, and its degraded fragments, iC3b/C3dg, in the colonic mucosa of ulcerative colitis (UC). Clin. Exp. Immunol. 104:286-292, 1996.
- Walport MJ. Complement. N. Engl. J. Med. 344:1058-1066, 2001.
- Walton J, Karpati G, Hilton-Jones D. Disorders of Voluntary Muscle. Churchill Livingstone, 769-771, 1994.
- Wenzel K, Zabojszeza J, Carl M, Taubert S, Lass A, Harris CL, Ho M, Schulz H, Hummel O, Hubner N, Osterziel KJ, Spuler S. Increased susceptibility to complement attack due to down-regulation of decay-accelerating factor/CD55 in dysferlin-deficient muscular dystrophy. J. Immunol. 175:6219-6225, 2005.
- Wong ML, Medrano JF. Real-time PCR for mRNA quantification. Biotechniques 39:75-85, 2005.
- Yazer MH, Judd WJ, Davenport RD, Dake LR, Lomas-Francis C, Hue-Roye K, Powell V, Reid M. Case report and literature review: transient Inab phenotype and agglutinating anti-IFC in a patient with a gastrointestinal problem. Transfusion 46:1537-1542, 2006.
- Zhou Y, Gong B, Lin F, Rother RP, Medof ME, Kaminski HJ. Anti-C5 antibody treatment ameliorates weakness in experimentally acquired myasthenia gravis. J. Immunol. 179:8562-8567, 2007.

APPENDIX A – General Recipes and Reagents

Amplification of DNA constructs

Luria broth (LB)

10g Bacto-tryptone
5g Yeast extract
10g Sodium Chloride
Make up to 1 litre with dH_20
Autoclave and store at room temperature

LB agar

100g Bacto-tryptone
5g Yeast extract
10g Sodium chloride
15g agar
Make up to 1 litre with dH_20
Autoclave and store at room temperature

Gel electrophoresis

2% Agarose gel

1g agarose powder
50ml 1xTBE
Heat solution to dissolve agarose
Cool to approximately 50ºC
Pour and allow to set

10x Tris-Borate-EDTA (TBE) electrophoresis buffer

0.89M Tris
0.89M Boric acid
0.02M EDTA
Make up to 1 liter with dH_2O
For use, dilute to 1x

Agarose loading dye

0.25% bromophenol blue (0.125g)
40% sucrose (20g)
Make up to a final volume of 50ml with dH_20

SYBR gold

Make a 1 in 2000 of loading dye

RNA extraction

DEPC-treatment

0.1% DEPC in distilled water
Stir for 30 minutes
Soak pipette tips and micro-centrifuge tubes in DEPC-treated water overnight
Remove as much as possible and autoclave

Tissue culture

Penicillin/Streptomycin

900mg penicillin
1500mg streptomycin
Make up to 150ml in 1x PBS
Filter trough 0.22µM filter
Store at -20ºC

Trypsin-EDTA

8g NaCl
1.26g Na_2HPO_4
0.2g KCl
0.2g KH_2PO_4
0.5G Trypsin
0.2g EDTA
Make up to 1 liter with dH_2O
pH to 7.4
Filter sterilize through 0.22 µM filter
Store at 4 ºC

Western blot

30:08 Acrylamide:bisacrylamide

30g acrylamide
0.8g N-N-methylene bisacrylamide
Make up to 100ml with dH_20
Store at 4ºC covered in foil

10% Ammonium persulphate (APS)

0.1g ammonium persulphate
Make up to 1ml with dH_20

10% Sodium dodecyl sulphate (SDS)
100g SDS
Make up to 1 liter with dH_20
pH to 7.2
Store at room temperature

Antibodies (Primary)
BRIC216 Mouse monoclonal anti-DAF 1 in 100 in 5% skim milk
P38 Rabbit polyclonal
1 in 5000 in 1x PBS/0.1% Tween

Antibodies (Secondary)
Goat anti-mouse IgG HRP conjugated
1 in 5000 in 5% skim milk
Goat anti-rabbit IgG HRP conjugated
1:5000 in skim milk

5% Blocking buffer
5% powder skim milk (w/v)
Make up to 50ml with 1x PBS/0.1% Tween

10x Running buffer
40g Glycine
63.2g Tris
10g SDS
Make up to 1 liter with dH_20
For use, dilute to 1x

10x Transfer buffer
144g Glycine
38g Tris
Make up to 1 liter with dH_20

1x Transfer buffer
100ml 10x transfer buffer
700ml dH_20
200ml isopropanol
Mix well with magnetic stirrer
Store at 4ºC

Membrane stripping buffer
100mM β-mercaptoethanol
2% SDS
62.5mM Tris-HCl pH6.7

10x Phosphate Buffered Saline (PBS)
80g NaCl
26.8g $Na_2HPO_4.12H_2O$
2g KCl
2.4g KH_2PO_4
Make up to 1 liter, pH to 6.9 and autoclave
For use, dilute to 1x

1x PBS/0.1% Tween
1x PBS made up to 1 liter
1ml Tween
Stir for half an hour with stirrer bar

10x Protease inhibitor
1 protease inhibitor tablet (Roche, Germany)
2.5ml PBS

5x Protein loading dye for non-reducing conditions
10% glycerol
0.25M Tris-Cl pH 6.8
3mg Bromophenol blue
Store at room temperature

Non-reducing protein extraction buffer
150mM NaCl
1.0% NP-40 (Triton X-100 can be substituted for NP-40)
50mM Tris, pH8.0
Store at 4ºC

Extraction buffer for protein harvesting
Per 1ml of extraction buffer:
25x Complete protease inhibitor cocktail
1mg/ml Apoprotinin
100mM PMSF
1mg/ml Pepstatin

8% Resolving SDS-PAGE (10ml)
2.7ml 30% Acrylamide:bis
2.5ml 1.5M Tris (pH8.8)
100µl 10% SDS
100µl 10% APS
6µl TEMED
4.6ml dH_2O

5% Stacking gel (4ml)
650µl 30% Acrylamide:bis
500µl 1.5M Tris (pH6.8)
40µl 10% SDS
40µl 10%APS
4µl TEMED
2.75ml dH_2O

APPENDIX B – Molecular weight markers

GelPilot 100bp Plus (QIAGEN, USA)

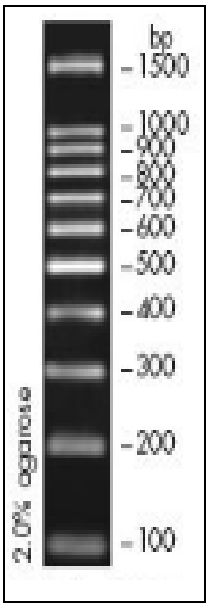

peqGold Prestained Protein Marker IV (PeqLab Biotechnologie, Germany)

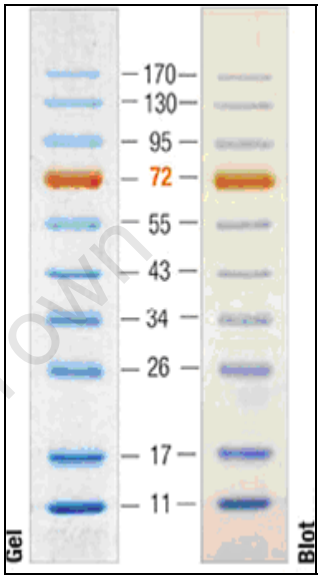

APPENDIX C – Protocol for establishing the standard curve (used gDAF as an example)

The equations given below were used to calculate the number of moles that contain $1x10^6$ molecules/mol:
Avogadro's number = 6.022×10^{23} molecules per mole
Pmoles of dsDNA = $\frac{\text{(ug dsDNA) (1515)}}{\text{Produce size in bp}}$

We calculate the number of moles that contain $1x10^6$ molecules as follows:

$\frac{1x10^6 \text{ molecules}}{6.022 \times 10^{23} \text{ molecules per mole}}$
$= 1.66x10^{-18}$ moles
$= 1.66x10^{-6}$ pmoles
i.e. $1.66x10^{-6}$ pmoles contain $1x10^6$ molecules.

Since Pmoles of dsDNA = $\frac{\text{(ug dsDNA) (1515)}}{\text{Produce size in bp}}$

Then ug of dsDNA = $\frac{\text{(Pmoles of dsDNA) (Produce size in bp)}}{1515}$

Product of gDAF = 322bp

That is then ug of dsDNA = $\frac{\text{(1.66x10}^{-6}\text{ pmoles) (322)}}{1515}$

$= 3.528x10^{-7}$ ug of dsDNA

$= 3.528x10^{-4}$ ng of dsDNA

= 0.3528 pg of dsDNA

Therefore the purified standard PCR product for gDAF was diluted to 0.3528 pg/µl to get $1x10^6$ molecules/µl.

APPENDIX D - Technical issues

Trouble-shooting and optimizing PCR amplification for the DAF promoter region

PCR amplification of *DAF* promoter region required optimization by trying different methods and changing the reagents. Initially, the PCR reaction for this region was carried out using the *GoTaq polymerase* enzyme following the conditions stated in Chapter 2. The experiments produced good results but later, for no apparent reason, failed. Firstly, we used fresh reagents including the primers, dNTPs, buffer and sterile water, but without success. Secondly, we tried increasing the concentration of the DNA template, followed by increasing the concentrations of the dNTPs and the *GoTaq polymerase* but with no success. Thirdly, we ran duplicate PCR reactions using reagents and a machine from another laboratory, but still failed. Using an alternative *Bioline BioTaq polymerase* and buffer did not produce any better results. Finally, we optimized the PCR reactions by using Failsafe buffer (Epicentre Biotechnologies, USA) which contained the dNTPs, the $MgCl_2$ and the buffer already mixed.

qRT-PCR method for quantifying *DAF* mRNA

Initially we experienced problems obtaining a smooth peak for the melting curve for the GUS gene. We optimized this by increasing the amount of the primers and the cDNA template. The best results were achieved by also changing certain conditions such as reducing the amount of holding time during the cycling from 30 seconds to 5 seconds.

There are two ways in which qRT-PCR quantification can be performed as explained in Chapter 2. Initially, we used the relative quantification method using the 2^{-ddCT} calculation. However, we obtained varying results for *DAF* mRNA expression from healthy controls which complicated interpretation of results from the MG patients. An alternative and adjunct method is to construct standard curves for each gene (Chapter 3) using absolute amounts of the standard dilutions of one chosen template. Subsequently, every qRT-PCR run included

one standard dilution which made it possible for us to compare the experiments done at different times. The two methods of quantification gave us similar trend of the results.

Initially we used a second house keeping gene, GAPDH. However, similar results were obtained as with GUS house keeping gene.

Transient transfection experiment

C2C12 muscle cells were allowed to differentiate for a longer period of time so as to obtain mature muscle cells, a better representative of the tissue in which the MG condition occurs. These cells have been shown to start differentiating as soon as the serum is reduced in the medium and after 24 hours the cells start to fuse longitudinally resulting in long muscle fibers (Kubo, 1991). We experienced difficulties with reproducing results in the transfections of C2C12 cells that were allowed to differentiate for 10 days. From the few readings obtained, the luciferase activity in these cells was very low and no visible differences were observed between the WT- and Mut-*DAF*. This may have been as a result of the cells failing to contain the transfected DNA plasmid for so many days or that there was low transfection efficiency in these cells.

Western blot analysis

When we acquired the BRIC 216 DAF antibody (International Blood Group Reference Laboratory, UK) they did not provide clear conditions under which the antibody recognizes the DAF protein. Since most antibodies recognize reduced and denatured protein and are used under reducing and denaturing conditions, we firstly ran a denaturing SDS gel using reduced protein. We could not detect any protein under these conditions. We then tried to optimize this by varying the amounts of protein and also the concentration of the BRIC 216 antibody used to detect the DAF protein. Unfortunately, none of these conditions gave us any results.

The next experiment we tried was to run a non-reducing and non-denaturing gel. We extracted the protein using the non-reducing buffer which

excluded SDS, the samples were not heated and the loading dye did not contain and protein denaturing reagents such as SDS, ß-mecaptoethanol and DTT. Additionally, we prepared a non-denaturing gel and running buffer by leaving SDS out. However, no results were obtained from this experiment.

Finally, we discovered that the BRIC 216 antibody recognizes the DAF protein under nor-reducing condition (without ß-mecaptoethanol and DTT) but on a denaturing gel (with SDS). Under these conditions we were able to detect the DAF protein.